



# Tumor-infiltrating lymphocyte treatment for anti-PD-1-resistant metastatic lung cancer: a phase 1 trial

Benjamin C. Creelan<sup>1,11</sup>✉, Chao Wang<sup>1,11</sup>, Jamie K. Teer<sup>2</sup>, Eric M. Toloza<sup>1</sup>, Jiqiang Yao<sup>2</sup>, Sungjune Kim<sup>3</sup>, Ana M. Landin<sup>4</sup>, John E. Mullinax<sup>5</sup>, James J. Saller<sup>6</sup>, Andreas N. Saltos<sup>1</sup>, David R. Noyes<sup>3</sup>, Leighann B. Montoya<sup>7</sup>, Wesley Curry<sup>7</sup>, Shari A. Pilon-Thomas<sup>3</sup>, Alberto A. Chiappori<sup>1</sup>, Tawee Tanvetyanon<sup>1</sup>, Frederic J. Kaye<sup>8</sup>, Zachary J. Thompson<sup>1</sup>, Sean J. Yoder<sup>9</sup>, Bin Fang<sup>9</sup>, John M. Koomen<sup>9</sup>, Amod A. Sarnaik<sup>1</sup>, Dung-Tsa Chen<sup>2</sup>, Jose R. Conejo-Garcia<sup>1</sup>, Eric B. Haura<sup>1,11</sup> and Scott J. Antonia<sup>10,11</sup>

**Adoptive cell therapy using tumor-infiltrating lymphocytes (TILs) has shown activity in melanoma, but has not been previously evaluated in metastatic non-small cell lung cancer. We conducted a single-arm open-label phase 1 trial (NCT03215810) of TILs administered with nivolumab in 20 patients with advanced non-small cell lung cancer following initial progression on nivolumab monotherapy. The primary end point was safety and secondary end points included objective response rate, duration of response and T cell persistence. Autologous TILs were expanded ex vivo from minced tumors cultured with interleukin-2. Patients received cyclophosphamide and fludarabine lymphodepletion, TIL infusion and interleukin-2, followed by maintenance nivolumab. The end point of safety was met according to the prespecified criteria of  $\leq 17\%$  rate of severe toxicity (95% confidence interval, 3–29%). Of 13 evaluable patients, 3 had confirmed responses and 11 had reduction in tumor burden, with a median best change of 35%. Two patients achieved complete responses that were ongoing 1.5 years later. In exploratory analyses, we found T cells recognizing multiple types of cancer mutations were detected after TIL treatment and were enriched in responding patients. Neoantigen-reactive T cell clonotypes increased and persisted in peripheral blood after treatment. Cell therapy with autologous TILs is generally safe and clinically active and may constitute a new treatment strategy in metastatic lung cancer.**

Despite progress with PD-1 immune-checkpoint inhibitors in metastatic lung cancer, the majority of patients fail to achieve an objective response<sup>1</sup>. Even when combined with first-line platinum-doublet chemotherapy, most patients suffer cancer progression within 12 months<sup>2</sup>. While substantial effort is currently dedicated toward identifying new immune-checkpoint combination partners, the clinical results thus far have been incremental<sup>3</sup>. One limitation of current combination approaches is that non-small cell lung cancers (NSCLCs) are often immunologically ‘cold’ tumors, with a paucity of activated, tumor-specific T cells<sup>4</sup>. Therefore, more effective combination immunotherapy is needed for metastatic NSCLC.

To address this challenge, adoptive cell therapy (ACT) using either autologous or allogeneic T cells is a potent strategy. In ACT, patients receive an infusion of a large number of T cells with tumor specificity. ACT using TILs cultured from a patient’s tumor has caused durable complete responses in a subset of patients with metastatic melanoma<sup>5</sup>. A hallmark of this therapy is the possibility

for durable remissions that can last for decades, due in part to the trans-differentiation potential and lifespan of memory T cells. Durable regressions with TILs have also previously been reported in a variety of epithelial malignancies, including cholangiocarcinoma<sup>6</sup>, cervical<sup>7</sup>, colorectal<sup>8</sup> and breast cancer<sup>9</sup>; however, this approach has not been evaluated in metastatic lung cancer.

Ex vivo expansion of TILs can release T cells from a suppressive microenvironment and reactivate them to target the tumor. By this method, billions of activated T cells can be produced and infused back into a patient. In contrast, T cells transduced with recombinant monoclonal receptors such as chimeric antigen receptors (CARs) or recombinant T cell receptors (TCRs) have met with problems in solid tumors, including absence of stable tumor antigen expression and the need for human leukocyte antigen (HLA) restriction. Toxicity can be severe and unpredictable, due to cross-reactivity or trace expression of tumor-associated antigens in normal epithelial or neural tissue<sup>10,11</sup>. Even if a clinical response is observed, acquired resistance is frequently conferred within several months<sup>12,13</sup>.

<sup>1</sup>Department of Thoracic Oncology, H. Lee Moffitt Cancer Center & Research Institute, Tampa, FL, USA. <sup>2</sup>Department of Bioinformatics and Biostatistics, H. Lee Moffitt Cancer Center & Research Institute, Tampa, FL, USA. <sup>3</sup>Department of Immunology, H. Lee Moffitt Cancer Center & Research Institute, Tampa, FL, USA. <sup>4</sup>Cell Therapy Facility, H. Lee Moffitt Cancer Center & Research Institute, Tampa, FL, USA. <sup>5</sup>Department of Sarcoma, H. Lee Moffitt Cancer Center & Research Institute, Tampa, FL, USA. <sup>6</sup>Department of Pathology, H. Lee Moffitt Cancer Center & Research Institute, Tampa, FL, USA. <sup>7</sup>Immune and Cellular Therapy Program, H. Lee Moffitt Cancer Center & Research Institute, Tampa, FL, USA. <sup>8</sup>Department of Medicine, University of Florida College of Medicine, Gainesville, FL, USA. <sup>9</sup>Chemical Biology & Molecular Medicine, H. Lee Moffitt Cancer Center & Research Institute, Tampa, FL, USA. <sup>10</sup>Duke Cancer Institute, Duke University School of Medicine, Durham, NC, USA. <sup>11</sup>These authors contributed equally: Benjamin C. Creelan, Chao Wang, Eric B. Haura, Scott J. Antonia. ✉e-mail: [ben.creelan@moffitt.org](mailto:ben.creelan@moffitt.org)

This may be due to deletion or mutation of the requisite antigen, antigenic heterogeneity<sup>14</sup> or impaired trafficking<sup>15</sup>. In contrast to recombinant monoclonal technology such as CARs, TILs are composed of polyclonal cells capable of targeting multiple tumor antigens. As TILs are derived from native genetically unmodified cells, complications due to engagement of normal host cells is uncommon<sup>16</sup>. As TILs have the potential to target ‘truncal’ neoantigens, which are clonally expressed by a cancer cell, resistance due to deficient target antigen expression may be less common<sup>17</sup>.

We hypothesized that TILs would be feasible and have clinical activity in metastatic NSCLC. Like melanoma, NSCLC also contains T cells that recognize tumor antigens<sup>18</sup>. Between 31–40% of patients with advanced NSCLC may have accessible metastatic supraclavicular adenopathy<sup>19–21</sup> and up to 40% have pleural metastases accessible through video-assisted thoracotomy<sup>22</sup>. Moreover, approximately 65% of patients with advanced NSCLC have pulmonary carbon monoxide diffusion capacity of  $\geq 50\%$  sufficient to tolerate the interstitial fluid shifts induced by interleukin (IL)-2 and lymphodepletion<sup>23</sup>. We also hypothesized that infused TILs could recognize antigens consisting of genomic alterations expressed by each individual patients’ tumor and that infused TIL clones may persist within peripheral blood.

We performed a phase 1 pilot trial of nivolumab followed by TILs in patients with metastatic NSCLC, with the primary end point of safety and secondary end points of response rate and survival. We collected tumors from patients who were naive to PD-(L)1 blockade, to reduce the proportion of terminally differentiated T cells in culture. Those with tumor enlargement or progression proceeded to receive TILs. We found that infusion of TILs in combination with lymphodepletion and IL-2 had manageable toxicity and mediated tumor regressions in several patients, including complete responses. We retrospectively screened whether expanded TILs were capable of reactivity to genomic alterations and identified that TILs were capable of recognizing a variety of types of cancer antigens.

## Results

**Patient characteristics.** Twenty patients were enrolled. Among them, 50% were current or former smokers. The median age was 54 years (range 38–75) and median PD-L1 proportion score was 6% (Supplementary Table 1). Forty percent were PD-L1 = 0% and 30% were PD-L1 > 50%. Median nonsynonymous tumor mutation burden (TMB) by whole-exome sequencing (WES) was 1.5 mutations per megabase of DNA (range 0.1–10.2). Four patients had epidermal growth factor receptor (*EGFR*) mutations, including two classical exon 19 deletions and two patients had *EML4-ALK* (anaplastic lymphoma kinase) translocations. The predominant enrolled histology was lung adenocarcinoma. One half of patients had not received previous systemic therapy. Most patients had bulky disease, with a mean sum of target lesion diameters of 8.5 cm before TIL treatment.

**Outcome after TIL collection and initial nivolumab.** Ninety percent of patients were discharged within 1 d or less after the excisional biopsy for TIL collection. Nivolumab treatment did not have any previously unreported adverse effects<sup>24</sup>. After excisional biopsy of their metastasis, all patients were treated with at least four cycles of intravenous nivolumab at a dose of 240 mg every 2 weeks (Fig. 1a). If patients had evidence of clinical benefit after two sequential computed tomography (CT) scans, then nivolumab was continued until progression. If there was evidence of progression, as defined by tumor enlargement or new lesions, then we proceeded to administer lymphodepletion and TIL treatment. At least two sequential CT scans were required to reduce the possibility of confounding error due to pseudo-progression<sup>25</sup>. Sixteen patients had tumor enlargement or new lesions (Extended Data Fig. 1a). Three patients had eventual partial response or complete response with initial nivolumab and therefore nivolumab was continued.

Two of these patients with an initial nivolumab benefit eventually had biopsy-proven progression while on nivolumab (Extended Data Fig. 1b) and were subsequently treated with TILs.

**Feasibility of TIL expansion and infusion.** TILs were successfully expanded for 95% of patients to a median dose of 95 billion CD3<sup>+</sup> cells (range 4.3–175). Specific reactivity to autologous tumor cell suspensions was detected in oligoclonal TIL cultures within 13 of 18 patients, as determined by interferon (IFN)- $\gamma$  capture by enzyme-linked immunosorbent assay (ELISA). The autologous reactivity of individual patients is presented in Extended Data Fig. 2. Four patients did not receive TILs due to reasons outlined in Fig. 1b. In total, 16 patients received lymphodepletion chemotherapy with cyclophosphamide and fludarabine followed by TIL infusion and IL-2 for 5 d. All these patients received full course lymphodepletion chemotherapy without dose modification. All treated patients initiated infusional IL-2 and the majority (56%) received all planned doses (Extended Data Fig. 3b). Six patients remained as inpatients after completing cyclophosphamide and the median length of inpatient stay was 12 d with a range of 7–22 d (Extended Data Fig. 3c). Patients with smoking history seemed to have a longer inpatient recovery time.

**Safety and adverse events.** Adverse effects were primarily attributable to the lymphodepletion and IL-2 combination (Extended Data Fig. 4 and Table 1). Common nonhematologic adverse events included hypoalbuminemia, hypophosphatemia, nausea, hyponatremia and diarrhea. Although manageable for the majority of patients, two patients died before a response assessment (identifier (ID) 13 and 15). Both patients had deteriorated to Eastern Cooperative Oncology Group performance status 3 and were requiring supplemental oxygen before start of lymphodepletion. Patient 13 was an active smoker with severe right carotid stenosis and had an ischemic right middle cerebral artery stroke at home at day +12. Patient 15 was 75 years old, limited to a wheelchair and had metastases replacing 70% of his pulmonary parenchyma. As he continued to decline after TIL treatment, he transitioned to comfort care without a CT scan. After these patients, more stringent pre-lymphodepletion performance status criteria were added. According to prespecified criteria for the safety end point, these two events were defined as severe toxicities, with a final severe toxicity rate of 12.5%. Following lymphodepletion, patients recovered lymphoid and myeloid lineages (Extended Data Fig. 5), with neutrophil count recovering at median 7.5 d (range 4.7–20.6). The majority of treatment-emergent adverse events had resolved within 1 month after TIL treatment. After 6 months of maintenance nivolumab, one patient had severe thrombocytopenia (ID 16). This event resolved with corticosteroid taper and cessation of nivolumab. The adverse events of each individual patient is listed separately in Supplementary Appendix 1.

**Clinical activity.** Initial tumor regression occurred in the majority of patients (11 of 16) at the first CT scan performed 1 month after TIL ACT. Overall, the median best change in sum of target lesion diameters was –35.5% (range +20 to –100). Radiographic response, including unconfirmed response, occurred for 6 of 13 evaluable patients. These included two complete responses which remain ongoing 1.5 years later (Fig. 2a). Two patients had unconfirmed partial response due to subsequent new brain metastases (ID 02, 05) and another two patients maintained a clinical remission by local ablative therapy of a new ‘escape’ lesion (ID 03, 08) performed between 6 and 17 months after TIL infusion (Fig. 2b). Another patient (ID 14) had enlargement of her only target lesion and biopsy showed fibrosis tissue (Extended Data Fig. 6). As this was a core biopsy, we could not rule out the presence of occult tumor cells elsewhere in the lesion. She remained without disease-related symptoms

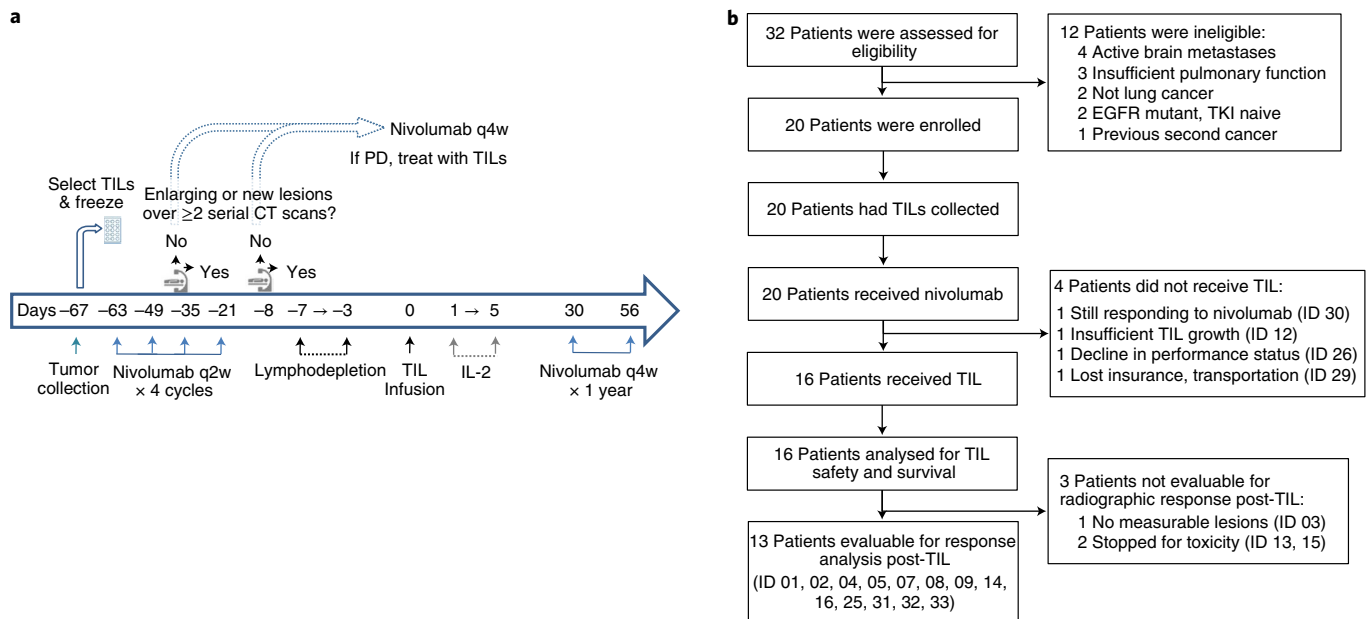


**Fig. 1 | Schematic representing study design and patient disposition.** **a**, Clinical trial schema. Day count is relative to TIL infusion. **b**, Patient disposition per Consolidated Standards of Reporting Trials guidelines. Of the 16 patients treated with TILs, 2 of them had initial response to nivolumab, followed by progressive disease before receiving TIL therapy. TKI, tyrosine kinase inhibitor; PD, progressive disease; q w, every week.

on trial for 1.5 years, before eventual progression with new lesions. Among 20 patients enrolled, median overall survival was not reached on an intention-to-treat basis (Extended Data Fig. 7) or after TIL treatment (Fig. 2d).

**Presence of T cells recognizing cancer mutations.** We sequenced whole-exomes and transcriptomes of pre-treatment tumors with paired germline and HLA sequencing (Supplementary Table 2). For each patient, we screened infused T cells for recognition of tumor nonsynonymous alterations, including indels and translocations. If aberrant cancer testis antigen was detected, these proteins were also screened. We selected between 13–100% of somatic variants for screening, with a median of 54 mutations per patient and range of 8 to 117. If the number of predicted neoantigens was >100, we limited the tested antigens to those with predicted peptide-major histocompatibility complex (pMHC) <500 nM<sup>26</sup>, confirmed mutation coverage and detectable RNA expression (fragments per kilobase of transcript per million mapped reads >0). In patients who did not have a research apheresis performed at day +30, we restricted testing to the highest priority neoantigens due to limited cell samples. A summary of how antigens were selected is included in Supplementary Table 3. Custom-synthesized peptide pools were pulsed with autologous antigen-presenting cells (APCs). For each ELISpot assay, co-culture of T cells and APCs, but without peptides, was used as a negative control and a one-way analysis of variance with Dunnett's multiple comparison test was used to determine whether the peptide elicited reactivity relative to control. We considered peptides as TIL-recognized peptides if  $P < 0.05$ . If peptides displaying tumor genomic alterations were confirmed as eliciting T cell reactivity, then these were co-cultured with autologous APCs and T cells over 10 d. A summary of all detected neoantigens is shown as a Supplementary Table 4.

One patient with *EGFR*<sup>ΔEx19</sup> lung adenocarcinoma (ID 25) had cancer refractory to nivolumab, yet achieved a sustained complete response after TIL treatment (Fig. 3a). Her infused TILs contained not only T cell clonotypes capable of recognizing one somatic mutation, but also several melanoma-associated gene (MAGE) cancer testis antigens discovered to be aberrantly expressed in her

tumor (Fig. 3b). Using post-TIL peripheral blood T cells, we used an antigen-recognition method to evaluate in vitro expansion of T cell clones after peptide stimulation<sup>27</sup>. Nineteen T cell clonotypes exhibited antigen-specific stimulation (Extended Data Fig. 8a), with mean 140-fold expansion relative to controls. There was a marked increase in these T cell clonotypes circulating in peripheral blood at post-infusion time points, which persisted >1 year (Fig. 3c). Another patient (ID 09) had a complete response to TILs after progressing with a new biopsy-proven soft tissue metastasis while on initial nivolumab (Fig. 3d). Three mutations elicited reactivity from both CD4<sup>+</sup>- and CD8<sup>+</sup>-sorted TILs (Fig. 4e) and peripheral blood T cells. Like patient 25, a similar surge in antigen-linked T cell clonotypes occurred after TIL infusion within peripheral blood (Fig. 3f and Extended Data Fig. 8b). This effect was not evident with nivolumab alone, despite an initial partial response. Another patient (ID 16) with a confirmed partial response had antigens targeting aberrant expression of MAGE-A4. Notably, clinical responses were associated with polyclonal T cell responses against neoantigens derived from a variety of genetic alterations, including single nucleotide variants, insertions/deletions and gene fusions, in addition to cancer testis antigens (Fig. 4). However, specific antigens could not be found in some patients. In an exploratory comparison, T cells functionally recognizing aberrant tumor antigens were identified in most patients who achieved an unconfirmed partial response, partial response or complete response after TIL treatment compared to nonresponders ( $P = 0.02$ , Fisher's exact test).

**Persistence and phenotype of T cells.** We characterized infused T cells for markers of terminal differentiation, which can be an indirect sign of impaired function or persistence. We performed flow cytometry upon retained aliquots from the final infused TIL product and detected high expression of several immune-checkpoint ligands, as shown in Extended Data Fig. 9a. In particular, all TILs had high expression of T cell immunoglobulin and mucin-domain-containing 3 (Tim-3) and T cell immunoreceptor with Ig and ITIM domains (TIGIT). Cell surface expression of both Tim-3 and TIGIT receptors is known to inhibit type 1 helper T cell-mediated immune responses and promote tolerance.

**Table 1 | Treatment-emergent adverse events reported with cyclophosphamide, fludarabine, TILs or IL-2**

NCI CTCAE preferred term	Grade					
	1	2	3	4	5	Any
Lymphocyte count decreased	0 (0%)	0 (0%)	0 (0%)	16 (100%)	0 (0%)	16 (100%)
White blood cell count decreased	0 (0%)	0 (0%)	1 (6%)	15 (94%)	0 (0%)	16 (100%)
Anemia	1 (6%)	2 (13%)	13 (81%)	0 (0%)	0 (0%)	16 (100%)
Platelet count decreased	0 (0%)	1 (6%)	3 (19%)	11 (69%)	0 (0%)	15 (94%)
Neutrophil count decreased	0 (0%)	2 (13%)	1 (6%)	11 (69%)	0 (0%)	14 (88%)
Hypoalbuminemia	0 (0%)	13 (81%)	1 (6%)	0 (0%)	0 (0%)	14 (88%)
Nausea	7 (44%)	7 (44%)	0 (0%)	0 (0%)	0 (0%)	14 (88%)
Hypophosphatemia	0 (0%)	4 (25%)	8 (50%)	0 (0%)	0 (0%)	12 (75%)
Hyponatremia	8 (50%)	0 (0%)	2 (13%)	1 (6%)	0 (0%)	11 (69%)
Hypocalcemia	6 (38%)	2 (13%)	2 (13%)	0 (0%)	0 (0%)	10 (63%)
AST increased	6 (38%)	1 (6%)	2 (13%)	0 (0%)	0 (0%)	9 (56%)
Fever	3 (19%)	5 (31%)	1 (6%)	0 (0%)	0 (0%)	9 (56%)
Diarrhea	5 (31%)	4 (25%)	0 (0%)	0 (0%)	0 (0%)	9 (56%)
Rash	7 (44%)	2 (13%)	0 (0%)	0 (0%)	0 (0%)	9 (56%)
Hypoxia	1 (6%)	5 (31%)	2 (13%)	0 (0%)	0 (0%)	8 (50%)
Dyspnea	1 (6%)	6 (38%)	1 (6%)	0 (0%)	0 (0%)	8 (50%)
ALP increased	5 (31%)	2 (13%)	1 (6%)	0 (0%)	0 (0%)	8 (50%)
Sinus tachycardia	3 (19%)	5 (31%)	0 (0%)	0 (0%)	0 (0%)	8 (50%)
ALT increased	5 (31%)	3 (19%)	0 (0%)	0 (0%)	0 (0%)	8 (50%)
Hyperkalemia	6 (38%)	0 (0%)	0 (0%)	1 (6%)	0 (0%)	7 (44%)
Hypotension	2 (13%)	4 (25%)	1 (6%)	0 (0%)	0 (0%)	7 (44%)
Chills	6 (38%)	1 (6%)	0 (0%)	0 (0%)	0 (0%)	7 (44%)
Anorexia	3 (19%)	3 (19%)	0 (0%)	0 (0%)	0 (0%)	6 (38%)
Edema limbs	3 (19%)	3 (19%)	0 (0%)	0 (0%)	0 (0%)	6 (38%)
Creatinine increased	3 (19%)	1 (6%)	1 (6%)	0 (0%)	0 (0%)	5 (31%)
Prothrombin time (INR) increased	4 (25%)	1 (6%)	0 (0%)	0 (0%)	0 (0%)	5 (31%)
Vomiting	1 (6%)	4 (25%)	0 (0%)	0 (0%)	0 (0%)	5 (31%)
Hypermagnesemia	5 (31%)	0 (0%)	0 (0%)	0 (0%)	0 (0%)	5 (31%)
Dysphagia	3 (19%)	1 (6%)	0 (0%)	0 (0%)	0 (0%)	4 (25%)
Dry mouth	4 (25%)	0 (0%)	0 (0%)	0 (0%)	0 (0%)	4 (25%)
Hypokalemia	4 (25%)	0 (0%)	0 (0%)	0 (0%)	0 (0%)	4 (25%)
Pulmonary edema	0 (0%)	2 (13%)	0 (0%)	1 (6%)	0 (0%)	3 (19%)
Hyperglycemia	1 (6%)	1 (6%)	1 (6%)	0 (0%)	0 (0%)	3 (19%)
Respiratory term, not otherwise specified	0 (0%)	3 (19%)	0 (0%)	0 (0%)	0 (0%)	3 (19%)
Weight loss	0 (0%)	3 (19%)	0 (0%)	0 (0%)	0 (0%)	3 (19%)
Dehydration	2 (13%)	1 (6%)	0 (0%)	0 (0%)	0 (0%)	3 (19%)
Dizziness	2 (13%)	1 (6%)	0 (0%)	0 (0%)	0 (0%)	3 (19%)
Mucositis oral	2 (13%)	1 (6%)	0 (0%)	0 (0%)	0 (0%)	3 (19%)
Febrile neutropenia	3 (19%)	0 (0%)	0 (0%)	0 (0%)	0 (0%)	3 (19%)

Shown are all adverse events (n, %) of the highest grade recorded for all TIL treated patients (n=16) with possible, probable and definite attribution for any of the trial treatment drugs cyclophosphamide, fludarabine, TILs or IL-2 occurring in >2 patients. ALP, alkaline phosphatase; ALT, alanine aminotransferase; AST, aspartate aminotransferase; INR, international normalized ratio; NCI CTCAE, National Cancer Institute Common Terminology Criteria for Adverse Events v.4.

Moreover, several patients had a high proportion of cells classified as regulatory T cells (Extended Data Fig. 9b). We performed *t*-distributed stochastic neighbor embedding (*t*-SNE) of memory differentiation markers based on lineage-specifying transcription factors and TIL differentiation status was primarily composed of CCR7<sup>-</sup>CD45RA<sup>-</sup> T effector memory cells<sup>28</sup> (Extended Data Fig. 9c). This predominance of terminally differentiated cells was likely due

to the  $\geq 7$  total weeks of accrued time in culture medium under chronic IL-2 stimulation.

Patients achieved durable conversion of the phenotype of their peripheral T cells after TIL infusion. This effect was not evident from initial nivolumab alone. In particular, we compared the ability of T cells to secrete cytokine proteins, derived before and after TIL infusion. We assessed the polyfunctional strength index (PSI),

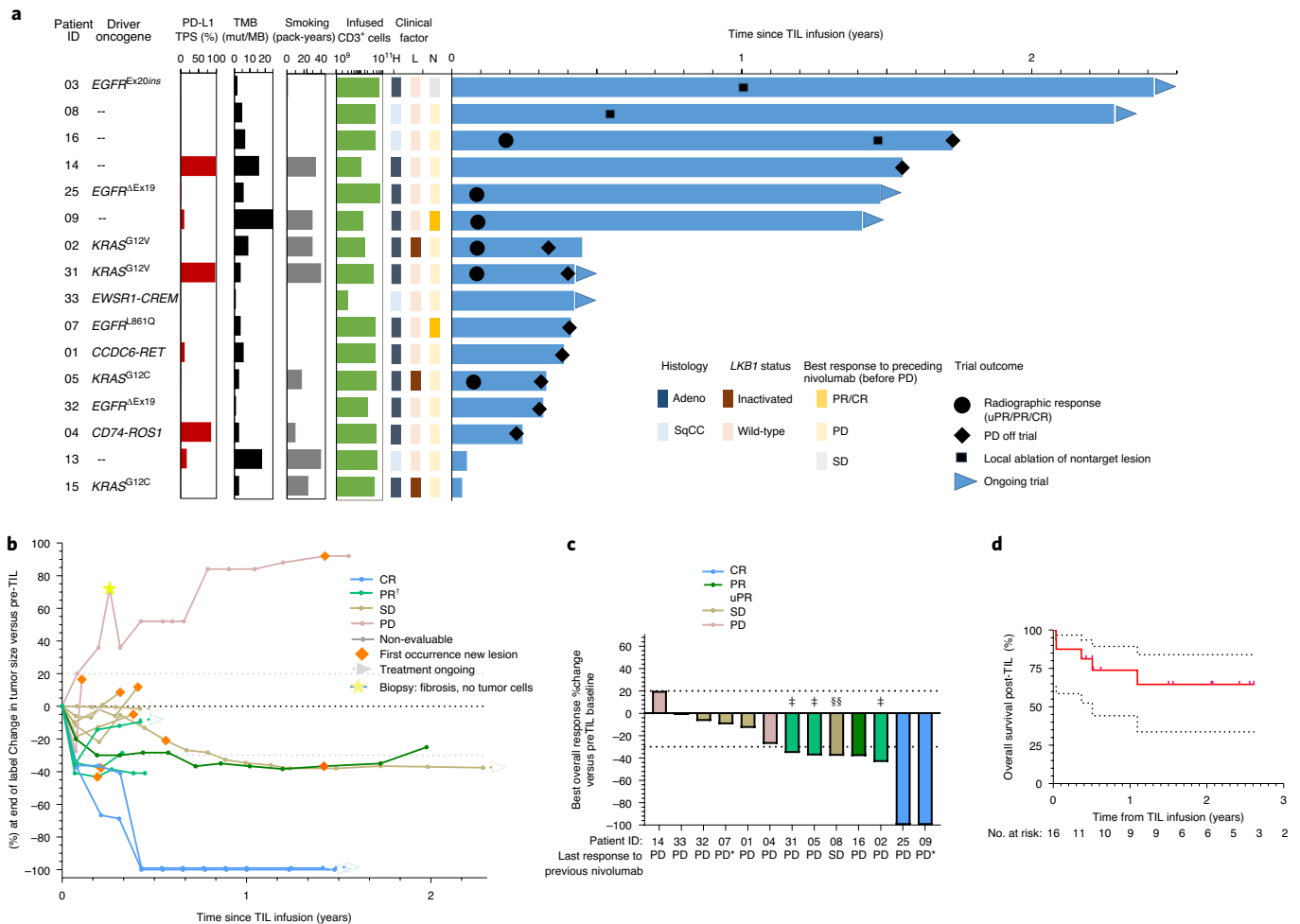


**Fig. 2 | Clinical activity of TILs and patient survival. a**, Features of patients who were treated with TILs and their clinical outcomes ( $n = 16$ ). **b**, Change in sum of tumor diameters, relative to week  $-1$  before TIL treatment. Nonevaluable patients (ID 03, 13, 15) are not shown. Patient 14, designated as radiographic ‘PD’ post-TIL, had biopsy of only the target lesion, showing fibrosis with no tumor cells at the time of progression. **c**, Waterfall plot showing best overall change in sum of diameter of tumor lesions. Change in sum of tumor diameters by RECIST is compared to week  $-1$  before TIL treatment. RECIST, Response Evaluation Criteria in Solid Tumors. Patient 14, designated as radiographic ‘PD’ post-TILs, had biopsy showing only the target lesion with fibrosis with no tumor cells. All patients evaluable with a post-TIL CT scan are included ( $n = 13$ ). Nonevaluable patients (ID 03, 13, 15) are not shown. ‘\*’ denotes initial PR with nivolumab, followed by biopsy-proven unequivocal PD (ID 07, 09); ‘‡’ denotes unconfirmed PR, subsequent nontarget PD (ID 02, 05, 31); ‘§§’ denotes patient with 10 mm increase in target lesion on previous nivolumab (ID 08). **d**, Overall survival of all treated patients from date of TIL infusion ( $n = 16$  patients). Hashtags denote 95% confidence intervals. Median follow-up of 1.6 years (range 0.5–2.9) by reverse Kaplan-Meier method. CR, complete response; PR, partial response; SD, stable disease; TPS, tumor proportion score by 22C3 antibody immunohistochemistry; TMB, tumor mutation burden; mut/MB, mutations per megabase; uPR, unconfirmed partial response. ‘Ex’ denotes exon and  $\Delta$  denotes exon deletion. Smoking pack-years represents self-reported cigarette packs per day multiplied by total years.

which is an indicator of the number of cells capable of secreting multiple types of cytokines. As PSI reflects the ability of a T cell to carry out multiple functions, it is recognized as a metric for the potency of cell therapy and for the efficacy of vaccines<sup>29</sup>. We performed a single-cell assay of 12 cytokines, testing up to 1,000 individual CD8<sup>+</sup> and CD4<sup>+</sup> cells after stimulation with CD28 antibody, relative to normalized background levels of each protein. PSI was increased at post-infusion time points after TIL treatment (Fig. 5a). Likewise, peripheral T cells changed to an effector memory (T<sub>EM</sub>) lineage characteristic of the infused TIL product for CD8<sup>+</sup> and CD4<sup>+</sup> cells, followed by gradual recovery of naive T cell types (Fig. 5b). As this treatment effect upon the peripheral compartment was not limited to the lifespan of the infused T cell pool, it may have been related in part to immune reconstitution or persistence.

To address this question of persistence, we examined the complementarity-determining regions of the T cell receptor  $\beta$ -chain

(TRV- $\beta$ ) over time. Each receptor motif is unique to a clonal population of cells and reflects the total number of each clone in circulation. We performed TRV- $\beta$  sequencing on snap-frozen tumor and serial peripheral blood samples for patients. We found the infused TIL clonotypes largely partially replaced the patients’ baseline peripheral T cell repertoire and then gradually decayed in proportion over the ensuing months (Fig. 5c). No apparent association between TIL clonotype systemic persistence and response was observed. Likewise, in an exploratory comparison, no clear association between radiographic response and either infused cell dose or autologous tumor reactivity of TILs was evident (Extended Data Fig. 10). There was also no discernable differences in the yield of TIL final cell count based on previous lines of treatment. TIL cultures did undergo change in clonotypic composition, with apparent enrichment of T cell clones in several patients during TIL culture compared to baseline tumor (Extended Data Fig. 10c). This enrichment

may have been due in part to antigen-driven expansion of T cells in culture, although the specificity of the clonotypes was unknown. This was accompanied by turnover in the most prevalent T cell clonotypes, possibly related to either clonal selection or stochastic drift (Extended Data Fig. 10d). Overall, TIL cultures were more clonal and less diverse than the baseline intratumoral T cells (median 6% versus 31%,  $P < 0.0001$ ; Extended Data Fig. 10e). We concluded the final infused TIL composition was not simply a scaled up reproduction of the original T cells resident within the collected tumor of each patient. Instead, TILs underwent clonal contraction within culture, which may have impaired the polyvalence and ultimate efficacy of the cell product.

## Discussion

We found that excisional tumor biopsy and nivolumab followed by administration of cyclophosphamide, fludarabine, IL-2 with TIL infusion in pretreated metastatic lung cancer was feasible in an academic center setting and had manageable adverse effects. We observed that lymphocytes could be successfully expanded from most patients' tumors and were largely capable of autologous tumor recognition. In addition to two durable complete responses, we also observed some patients who derived clinical benefit in a variety of other ways, including local ablation of a single metachronous new lesion. One durable complete response occurred in a TMB<sub>low</sub>, PD-L1<sub>negative</sub> never-smoker, who was refractory to nivolumab. This may be particularly encouraging for the large subset of never-smoker patients, for whom immune-checkpoint inhibitors have historically had limited efficacy<sup>30</sup>. Although neoantigen load was predictive of clinical benefit in a small melanoma cohort treated with TILs<sup>31</sup>, it seems that infusion of T cells that target anti-tumor antigens is of particular importance. Together with results in breast cancer<sup>9</sup>, our data indicate that TILs can mediate effective responses in tumor subtypes that are not sensitive to traditional immune-checkpoint-targeted therapy. Therefore, therapy with TILs may extend the scope and impact of immunotherapy into wider populations.

Our report adds to growing evidence that TIL ACT may be active in a variety of epithelial malignancies. In contrast to previous experience in melanoma, we found a high proportion of CD4<sup>+</sup> TILs in NSCLC. Despite this, CD4<sup>+</sup>-predominant TILs were capable of mediating responses and antigen-specific CD4<sup>+</sup> clones recognizing immunogenic tumor mutations were identified (Fig. 3). Antigen-specific CD4<sup>+</sup> cells recognizing mutations such as *BRAF*<sup>V600E</sup> have previously been identified in melanoma<sup>32</sup> and have mediated tumor regressions in gastrointestinal malignancies<sup>33</sup>. Therefore, an important requirement for TIL efficacy may be the presence of sufficient T cells that recognize immunogenic genomic alterations. In our case, we found autologous T cells that were reactive to multiple types of tumor antigens (Fig. 4). Further study is needed to determine the threshold polyclonality or diversity of antigens targeted by an infused TIL repertoire, required to achieve a durable clinical response.

Although infusion of mutation-reactive T cells seems to be important for a successful TIL response, the lineage differentiation status of T cells may be paramount. CD8<sup>+</sup> T cells with stem-like surface markers were associated with tumor cytolysis and durability of responses in a large cohort of melanoma patients treated with TILs<sup>34</sup>. In fact, the majority of mutation-reactive T cells were terminally differentiated and not associated with clinical benefit. However, a small subset of mutation-reactive T cells were detected in the CD39<sup>-</sup>CD69<sup>-</sup> stem-like state and these were associated durable remission. Therefore, both specificity and lineage seem to be critical factors in melanoma and further study in NSCLC is warranted.

Lymphodepletion chemotherapy and IL-2 are prerequisites to ensure homeostatic expansion and engraftment of infused TILs. This incumbent toxicity, together with the required production infrastructure, has historically limited experimentation with TILs to select centers. We had two patients with early deaths related to worsening performance status and inanition caused by rapidly progressive disease, combined with physiologic stress of lymphodepletion and IL-2. By the time that TILs could be manufactured, these patients were infirm and requiring supplemental oxygen. Future strategies to expedite TIL manufacturing<sup>35</sup> and curtail the physiologic footprint of lymphodepletion may be needed to ensure the broader adoption of TILs in the lung cancer community. To this end, newer, less-invasive approaches to isolate and expand tumor neoepitope-reactive T cells are being pioneered to expand to indications with limited tumor access. For example, expansion of TILs is possible from core needle biopsies, with final product counts in the 1–10 billion cell range across a variety of epithelial malignancies<sup>36</sup>. This approach is currently being tested in registration trials (NCT04614103). PD-1<sup>+</sup> selection may enrich for neoantigen-reactive T cells from the peripheral blood of patients with melanoma and gastrointestinal cancer<sup>37</sup>. In ovarian cancer, tumor-reactive TILs are reported primarily in the PD-1<sup>+</sup> fraction of cells and a T cell-inflamed genetic signature or high TMB may also help to predict antitumor reactivity<sup>38</sup>. Likewise, sorting for memory T cell markers may capture most of the mutated neoantigen-reactive T cells in the peripheral blood of patients with epithelial cancer<sup>39,40</sup>.

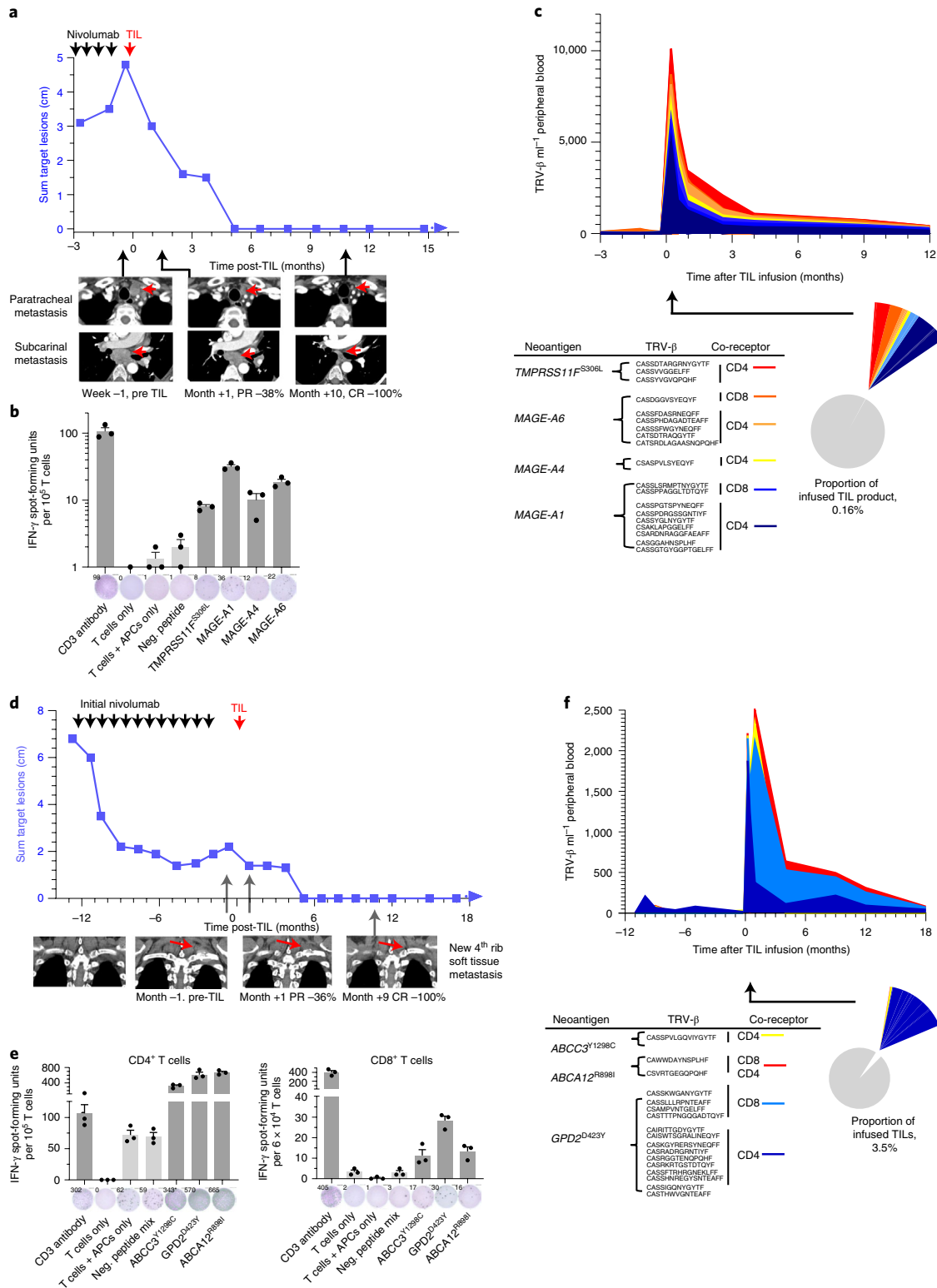
Our study was characterized by important limitations derived from its design. The completion of the trial within two academic cancer centers does not necessarily reflect feasibility of daily practice in a less-specialized setting. Along these lines, we enrolled a highly selected group with a larger-than-normal proportion of treatment-naïve, never-smoker and oncogene-addicted patients with lung cancer. This may have diminished the external validity of our results, because severe adverse events may be more frequent in patients with smoking-related diseases who are encountered in common practice. Within this combination therapy, the individual component contributions of IL-2, cyclophosphamide, fludarabine and nivolumab are difficult to assess. To the best of our knowledge, neither lymphodepletion nor IL-2 monotherapy have historically reported durable responses in NSCLC. In this trial, we gave initial nivolumab monotherapy in unselected patients with NSCLC, as a

**Fig. 3 | Examples of complete responses mediated by TIL-recognizing tumor antigens.** **a**, Patient 25, with an *EGFR*<sup>ΔE19</sup> tumor, had progressive metastases with nivolumab, followed by complete response to TILs. The sum of radiographic target lesions is shown over time with representative contrast-enhanced axial CT images. **b**, IFN- $\gamma$  spot formation after co-culture of her post-TIL T cells with her autologous DCs pulsed with synthesized long peptides displaying tumor antigens. Five proteins are shown, of 104 tested, mean  $\pm$  s.e.m. of three plates over two experiments. **c**, Absolute number of antigen-specific T cell receptor clonotypes within the peripheral blood after TIL treatment. The absolute number and proportion increased after TILs and then gradually decayed. Data are derived from a total of ten serial blood samples. The proportion of antigen-specific clones in her infused TIL product is shown in the pie chart. **d**, Patient 09 is a former smoker with lung adenocarcinoma. She had PR to nivolumab followed by enlargement of metastatic lymph nodes and a new biopsy-proven rib soft tissue metastasis 10 months later. She was then treated with TILs and had a CR with ongoing absence of radiographic target lesions. Representative coronal contrast-enhanced CT images are shown over time. **e**, Co-culture of either CD4<sup>+</sup> or CD8<sup>+</sup> T cells sorted from final infused TILs with autologous DCs and custom peptides corresponding to tumor neoantigens elicited reactivity. Three positive peptides are shown of 85 tested. Mean  $\pm$  s.e.m. of three plates over two experiments. **f**, Absolute number of antigen-specific clonotypes in peripheral blood increased and then gradually decayed after TIL infusion. Data are derived from a total of 13 serial blood samples. DCs, dendritic cells; Pt, patient.

trial alternative to a standard immune-checkpoint inhibitor and applicable chemotherapy. Patients were informed that nivolumab was not superior to standard chemotherapy<sup>41</sup>. Although uncorroborated, many patients opted for nivolumab followed by the prospect of cell therapy, due in part to interest in avoiding platinum-doublet chemotherapy and the historical experience of TILs in other cancers. Our trial included post-TIL nivolumab for up to 1 year, with the intent of deterring subsequent relapse related to PD-L1

expression. Nonetheless, the necessity or optimal duration of maintenance therapy after TIL therapy remains to be proven.

We chose to exclusively manufacture TILs from anti-PD-(L)1 treatment-naïve tumors. Exhausted TIL clones seem to have limited ability for phenotype transition to an activated state after PD-(L)1 blockade<sup>42</sup>. Therefore, we expected that pre-treatment tumor collection followed by PD-1 blockade would represent the most ideal scenario to test TIL efficacy, while still controlling for the effect of



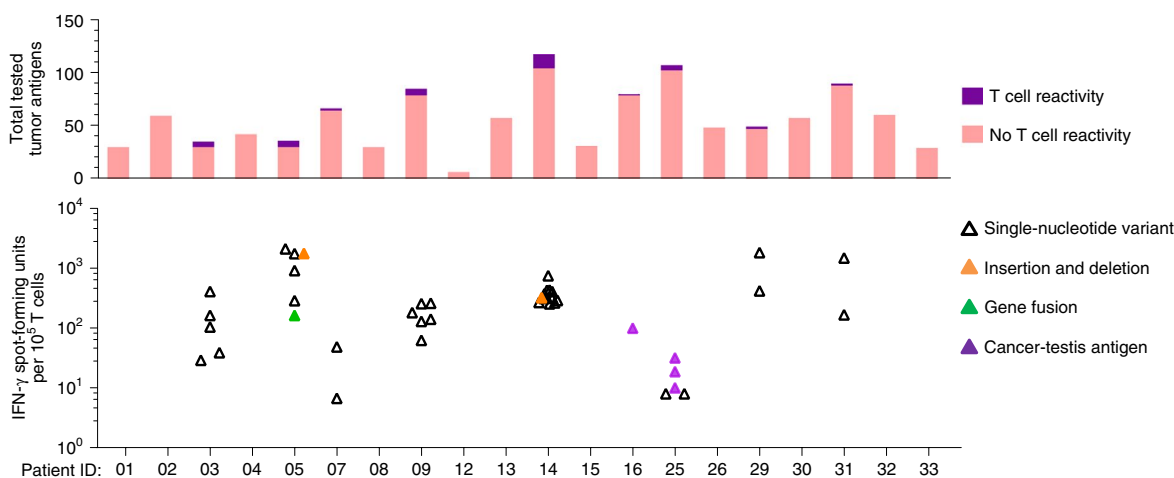


**Fig. 4 | Summary of tumor-specific antigens tested for all patients.** Total sum of unique genomic alterations tested for each patient (top). Tumor-specific antigens that were detected by autologous T cells (bottom). Positive antigens were assessed for T cell reactivity by synthesis of the corresponding recombinant peptides and identification of IFN- $\gamma$  colony formation by ELISpot, relative to controls with autologous T cells and DCs only. Mean spot-forming units per positive Ag are shown, with  $n=2-5$  tests per antigen. Cultured TILs were used to assess antigen reactivity for all patients except 02, 25, 32 and 33 due to high IFN- $\gamma$  background of cultured TILs. In these instances, autologous T cells isolated from post-TIL peripheral blood were used. Ag, antigen.

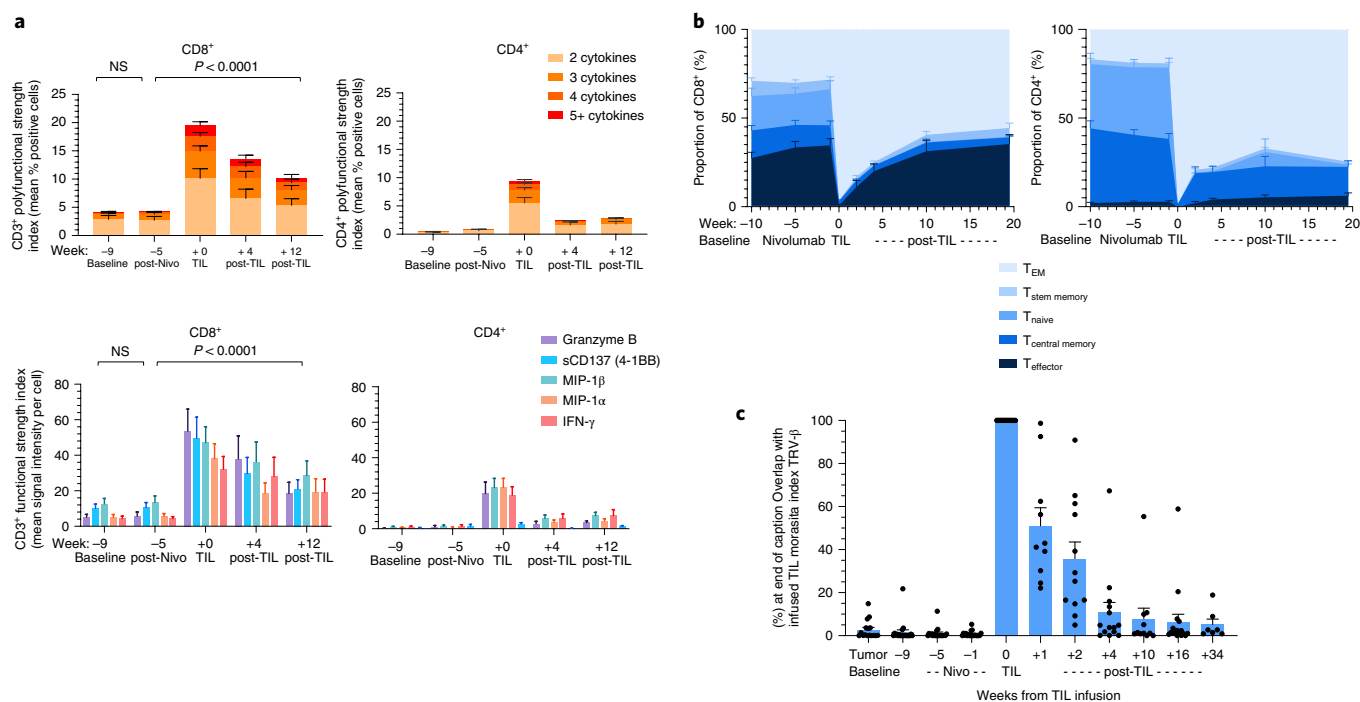


**Fig. 5 | Change in phenotype and genotype of peripheral T cells after TIL infusion.** **a**, Increase in circulating subsets of polyfunctional CD8<sup>+</sup> or CD4<sup>+</sup> T cells at post-infusion time points. \*Friedman test using mixed-effects model (REML) with stacked matching with Geisser–Greenhouse correction. Shown is the multiplicity adjusted, two-sided  $P$  value using Dunnett’s control for multiple comparisons, with family-wise  $\alpha$  of 0.05.  $P$  value = 0.0000008. Stacked bars denote mean  $\pm$  s.e.m. of available dataset with 12 tested patients. NS, not significant. **b**, Increase in peripheral CD45RA<sup>-</sup>CCR7<sup>-</sup> T<sub>EM</sub> cells at post-infusion time points for all patients with available time points ( $n=15$ ) with eight serial time points collected per patient. Stacked area curves denote mean  $\pm$  s.e.m. percentage of CD8<sup>+</sup> or CD4<sup>+</sup> T cells. Naive T cells are CD45RA<sup>+</sup>CCR7<sup>+</sup>CD95<sup>-</sup>; central memory cells are CCR7<sup>+</sup>CD45RA<sup>-</sup>; T<sub>EM</sub> are CCR7<sup>-</sup>CD45RA<sup>-</sup>; stem cell-like memory cells are CCR7<sup>+</sup>CD45RA<sup>+</sup>CD95<sup>+</sup>; and effector T cells are CCR7<sup>-</sup>CD45RA<sup>+</sup>. **d**, Overlap of TRV- $\beta$  chain productive rearrangements between final infused TIL product and peripheral blood T cells at indicated time points, using Morasita’s index. Bars denote mean  $\pm$  s.e.m. of all patients with available time points for analysis ( $n=16$ ). nivo, nivolumab; MIP, macrophage inflammatory protein; REML, restricted (or residual or reduced) maximum likelihood; CCR, chemokine receptor.

nivolumab monotherapy. In particular, one patient (ID 09) still had a complete response to TILs after suffering relapse after 1 year on nivolumab. This suggests that anti-PD-1 treatment-naïve TILs can

still mediate specificity and cytotoxicity against PD-1-experienced tumor cells. Despite the observation that bulk TILs expressed multiple immune-checkpoint proteins, we demonstrated that

neopeptide-specific T cells retained functionally capable of IFN- $\gamma$  secretion after antigen challenge. In a recent phase 2 trial of TILs for treatment refractory metastatic melanoma, 79% of responders had ipilimumab-refractory disease and all had previous PD-1 blockade, demonstrating that TILs still have efficacy for some patients after progression on immune-checkpoint inhibitors<sup>43</sup>. Based on its activity and safety profile, TILs are a rational therapy to further investigate for fit, motivated patients with metastatic NSCLC. Future TIL trials will ideally enroll either patients with NSCLC who have progressed after combination chemotherapy and immunotherapy or patients who are predicted to have a poor chance of response to traditional immune-checkpoint inhibitors. Larger trials are required to further define the optimal biomarkers of response and the efficacy of TIL collected from patients who have progressed on previous PD-(L)1-based treatments.

### Online content

Any methods, additional references, Nature Research reporting summaries, source data, extended data, supplementary information, acknowledgements, peer review information; details of author contributions and competing interests; and statements of data and code availability are available at <https://doi.org/10.1038/s41591-021-01462-y>.

Received: 20 December 2020; Accepted: 6 July 2021;  
Published online: 12 August 2021

### References

- Man, J., Millican, J., Mulvey, A., GebSKI, V. & Hui, R. Response rate and survival at key timepoints with PD-1 blockade versus chemotherapy in PD-L1 subgroups: meta-analysis of metastatic NSCLC trials. *JNCI Cancer Spectrum* <https://doi.org/10.1093/jncics/pkab012> (2021).
- Addeo, A., Banna, G. L., Metro, G. & Di Maio, M. Chemotherapy in combination with immune checkpoint inhibitors for the first-line treatment of patients with advanced non-small cell lung cancer: a systematic review and literature-based meta-analysis. *Front. Oncol.* **9**, 264 (2019).
- Hellmann, M. D. et al. Nivolumab plus ipilimumab in advanced non-small-cell lung cancer. *N. Engl. J. Med.* **381**, 2020–2031 (2019).
- Schoenfeld, A. J. & Hellmann, M. D. Acquired resistance to immune checkpoint inhibitors. *Cancer Cell* **37**, 443–455 (2020).
- Rosenberg, S. A. et al. Durable complete responses in heavily pretreated patients with metastatic melanoma using T-cell transfer immunotherapy. *Clin. Cancer Res.* **17**, 4550–4557 (2011).
- Tran, E. et al. Cancer immunotherapy based on mutation-specific CD4<sup>+</sup> T cells in a patient with epithelial cancer. *Science* **344**, 641–645 (2014).
- Stevanović, S. et al. Complete regression of metastatic cervical cancer after treatment with human papillomavirus-targeted tumor-infiltrating T cells. *J. Clin. Oncol.* **33**, 1543 (2015).
- Tran, E. et al. T-cell transfer therapy targeting mutant KRAS in cancer. *N. Engl. J. Med.* **375**, 2255–2262 (2016).
- Zacharakis, N. et al. Immune recognition of somatic mutations leading to complete durable regression in metastatic breast cancer. *Nat. Med.* **24**, 724–730 (2018).
- Duinkerken, C. W. et al. Sensorineural hearing loss after adoptive cell immunotherapy for melanoma using MART-1 specific T cells: a case report and its pathophysiology. *Otol. Neurotol.* **40**, e674–e678 (2019).
- Blumenschein, G. et al. 278 Phase I clinical trial evaluating the safety of ADP-A2M10 SPEAR T-cells in patients with MAGE-A10<sup>+</sup> advanced non-small cell lung cancer. *J. Immunother. Cancer* <https://doi.org/10.1136/jitc-2020-SITC2020.0278> (2020).
- Lu, Y.-C. et al. Treatment of patients with metastatic cancer using a major histocompatibility complex class II-restricted T-cell receptor targeting the cancer germline antigen MAGE-A3. *J. Clin. Oncol.* **35**, 3322 (2017).
- D'Angelo, S. P. et al. Antitumor activity associated with prolonged persistence of adoptively transferred NY-ESO-1 c259T cells in synovial sarcoma. *Cancer Discov.* **8**, 944–957 (2018).
- Xia, Y. et al. Treatment of metastatic non-small cell lung cancer with NY-ESO-1 specific TCR engineered-T cells in a phase I clinical trial: a case report. *Oncol. Lett.* **16**, 6998–7007 (2018).
- Haas, A. R. et al. Phase I study of lentiviral-transduced chimeric antigen receptor-modified T cells recognizing mesothelin in advanced solid cancers. *Mol. Ther.* **27**, 1919–1929 (2019).
- Yeh, S. et al. Ocular and systemic autoimmunity after successful tumor-infiltrating lymphocyte immunotherapy for recurrent, metastatic melanoma. *Ophthalmology* **116**, 981–989. e981 (2009).
- Kast, F., Klein, C., Umaña, P., Gros, A. & Gasser, S. Advances in identification and selection of personalized neoantigen/T-cell pairs for autologous adoptive T cell therapies. *OncoImmunology* **10**, 1869389 (2021).
- Renkvist, N., Castelli, C., Robbins, P. F. & Parmiani, G. A listing of human tumor antigens recognized by T cells. *Cancer Immunol. Immunother.* **50**, 3–15 (2001).
- Ahmed, M., Flannery, A., Daneshvar, C. & Breen, D. PET and neck ultrasound for the detection of cervical lymphadenopathy in patients with lung cancer and mediastinal lymphadenopathy. *Respiration* **96**, 138–143 (2018).
- Fultz, P. J. et al. Detection and diagnosis of nonpalpable supraclavicular lymph nodes in lung cancer at CT and US. *Radiology* **222**, 245–251 (2002).
- Niwa, H. et al. Patterns of mediastinal and supraclavicular metastases in apical invasive lung cancer—importance of supraclavicular lymph node dissection. *Nihon Kyobu Geka Gakkai* **42**, 1142–1147 (1994).
- Doebele, R. C. et al. Oncogene status predicts patterns of metastatic spread in treatment-naïve nonsmall cell lung cancer. *Cancer* **118**, 4502–4511 (2012).
- Guerra, J. L. L. et al. Changes in pulmonary function after three-dimensional conformal radiotherapy, intensity-modulated radiotherapy, or proton beam therapy for non-small-cell lung cancer. *Int. J. Radiat. Oncol. Biol. Phys.* **83**, e537–e543 (2012).
- Weber, J. S. et al. Safety profile of nivolumab monotherapy: a pooled analysis of patients with advanced melanoma. *J. Clin. Oncol.* <https://doi.org/10.1200/JCO.2015.66.1389> (2017).
- Katz, S. I. et al. Radiologic pseudoprogression during anti-PD-1 therapy for advanced non-small cell lung cancer. *J. Thorac. Oncol.* **13**, 978–986 (2018).
- Jurtz, V. et al. NetMHCpan-4.0: improved peptide-MHC class I interaction predictions integrating eluted ligand and peptide binding affinity data. *J. Immunol.* **199**, 3360–3368 (2017).
- Forde, P. M. et al. Neoadjuvant PD-1 blockade in resectable lung cancer. *N. Engl. J. Med.* **378**, 1976–1986 (2018).
- Golubovskaya, V. & Wu, L. Different subsets of T cells, memory, effector functions, and CAR-T immunotherapy. *Cancers* **8**, 36 (2016).
- Precopio, M. L. et al. Immunization with vaccinia virus induces polyfunctional and phenotypically distinctive CD8<sup>+</sup> T cell responses. *J. Exp. Med.* **204**, 1405–1416 (2007).
- Gainor, J. F. et al. EGFR mutations and ALK rearrangements are associated with low response rates to PD-1 pathway blockade in non-small cell lung cancer: a retrospective analysis. *Clin. Cancer Res.* **22**, 4585–4593 (2016).
- Lauss, M. et al. Mutational and putative neoantigen load predict clinical benefit of adoptive T cell therapy in melanoma. *Nat. Commun.* **8**, 1–11 (2017).
- Veatch, J. R. et al. Tumor-infiltrating BRAF V600E-specific CD4<sup>+</sup> T cells correlated with complete clinical response in melanoma. *J. Clin. Investig.* **128**, 1563–1568 (2018).
- Tran, E. et al. Immunogenicity of somatic mutations in human gastrointestinal cancers. *Science* **350**, 1387–1390 (2015).
- Krishna, S. et al. Stem-like CD8 T cells mediate response of adoptive cell immunotherapy against human cancer. *Science* **370**, 1328–1334 (2020).
- Simpson-Abelson, M., D'Arigo, K., Hilton, E., Fardis, M. & Chartier, C. 1053P Iovance generation-2 tumour-infiltrating lymphocyte (TIL) product is reinvigorated during the manufacturing process. *Ann. Oncol.* **31**, S720 (2020).
- Simpson-Abelson, M., D'Arigo, K., Hilton, E., Fardis, M. & Chartier, C. Expanding Iovance's tumor infiltrating lymphocytes (TIL) from core biopsies for adoptive T cell therapy using a 22-day manufacturing process. in *SITC Annual Meeting* (SITC, 2019).
- Gros, A. et al. Recognition of human gastrointestinal cancer neoantigens by circulating PD-1<sup>+</sup> lymphocytes. *J. Clin. Investig.* **129**, 4992–5004 (2019).
- Salas-Benito, D. et al. The mutational load and a T-cell inflamed tumour phenotype identify ovarian cancer patients rendering tumour-reactive T cells from PD-1<sup>+</sup> tumour-infiltrating lymphocytes. *Br. J. Cancer* <https://doi.org/10.1038/s41416-020-01218-4> (2021).
- Malekzadeh, P. et al. Antigen experienced T cells from peripheral blood recognize p53 neoantigens. *Clin. Cancer Res.* **26**, 1267–1276 (2020).
- Cafri, G. et al. Memory T cells targeting oncogenic mutations detected in peripheral blood of epithelial cancer patients. *Nat. Commun.* **10**, 1–9 (2019).
- Carbone, D. P. et al. First-line nivolumab in stage IV or recurrent non-small-cell lung cancer. *N. Engl. J. Med.* **376**, 2415–2426 (2017).
- Yost, K. E. et al. Clonal replacement of tumor-specific T cells following PD-1 blockade. *Nat. Med.* **25**, 1251–1259 (2019).
- Sarnaik, A. et al. Long-term follow up of lifileucel (LN-144) cryopreserved autologous tumor infiltrating lymphocyte therapy in patients with advanced melanoma progressed on multiple prior therapies. *J. Clin. Oncol.* **38**, 10006 (2020).

**Publisher's note** Springer Nature remains neutral with regard to jurisdictional claims in published maps and institutional affiliations.

© The Author(s), under exclusive licence to Springer Nature America, Inc. 2021

## Methods

**Patients.** From October 2017 to January 2020, we enrolled patients in a dual-center phase 1 investigator-initiated trial designed to test the feasibility of ACT with TILs (ClinicalTrials.gov NCT03215810). Eligible patients were adults with histologically proven stage 4 NSCLC who were not candidates for surgical resection for curative intent or a curative-intent radiation modality. Patients were required to have an accessible metastasis to procure for TILs with acceptable anticipated perioperative risk and also at least one separate additional measurable tumor lesion on CT. All patients were required to have received fewer than six previous lines of systemic therapy. Previous therapy could not have included a PD-1 or PD-L1 inhibitor. Patients were required to have sufficient cardiopulmonary function, including a cardiac stress test showing no reversible ischemia; adjusted diffusing capacity for carbon monoxide (DLCO) >50% of predicted as assessed by pulmonary function testing; and left ventricular ejection fraction >50% as assessed by multigated acquisition (MUGA) scan. Patients with active brain metastases, autoimmune conditions or acquired immunodeficiency were excluded. Active brain metastases were excluded due to concern regarding symptomatic central nervous system progression during the ≥63-d TIL production to infusion time. Patients were required to have adequate normal organ and marrow function, defined as hemoglobin ≥9 g/100 mL; absolute neutrophil count  $\geq 1.0 \times 10^9 \text{ l}^{-1}$  ( $\geq 1,000 \text{ mm}^{-3}$ ); platelet count  $\geq 100 \times 10^9 \text{ l}^{-1}$  ( $> 100,000 \text{ mm}^{-3}$ ); albumin  $\geq 2.5 \text{ g}/100 \text{ mL}$ ; prothrombin time, partial thromboplastin time, serum bilirubin, serum creatinine  $\leq 1.5 \times$  of the institutional upper limit of normal; and AST and ALT  $\leq 2.5 \times$  of the institutional upper limit of normal.

Patients with *EGFR* mutation or *ALK* translocation were allowed if they had progressed on  $\geq 1$  previous approved TKIs. Comprehensive exome sequencing was performed on the resected tumor obtained after enrollment. This step revealed an uncommon *EGFR*<sup>L861Q</sup> in patient 07 and a variant *EML4-ALK* in patient 12, which was not detected on cell-free DNA assay before enrollment. Full details on eligibility are provided in the [Supplementary Protocol](#) and at <https://ClinicalTrials.gov>.

**Study conduct.** This study was conducted at two academic medical centers in the United States. The primary end points were safety and feasibility. Key secondary end points were radiologic response rate and overall survival. Adverse events were recorded according to NCI CTCAE v.4.0. Tumors were assessed per RECIST, v.1.1. Patients were deemed eligible and enrolled after passing all screening procedures, before tumor resection.

**Study design.** After excisional biopsy of metastasis, patients were treated with four cycles of intravenous nivolumab at a dose of 240 mg every 2 weeks (Fig. 1a). If patients had evidence of clinical benefit after two sequential CT scans, then nivolumab was continued until progression. If there was evidence of progression, as defined by tumor enlargement or new lesions, then we proceeded to administer lymphodepletion and TIL treatment. TIL infusion was defined as day 0. Patients received lymphodepletion intravenously with cyclophosphamide at a dose of 60 mg kg<sup>-1</sup> daily for day -7 and -6 with fludarabine daily at a dose of 30 mg m<sup>-2</sup> of body surface area for days -7 to -3. Patients were then admitted to hospital and received TIL infusion on day 0, followed by continuous aldesleukin infusion beginning 12 h later at a dose of 18 million international units (MIU) m<sup>-2</sup> over 6 h, then 12 h and then 24 h followed by 4.5 MIU m<sup>-2</sup> over 24 h for three consecutive days<sup>44</sup>. Patients were discharged once they had  $> 1,000 \text{ cells } \mu\text{l}^{-1}$  peripheral neutrophils. CT scans were performed every 6 weeks and leukapheresis at week 4 to collect immune cells for functional studies. Then patients resumed nivolumab 480 mg every 4 weeks for up to 1 year. If patients had a single site of progressive tumor, this was formally recorded as progression. However, these patients were permitted to remain on trial after successful local ablative therapy using either resection or stereotactic radiation. Oral prophylaxis for pneumocystis and herpes simplex virus was given for 6 months after TIL treatment.

**Study supervision.** This study was approved by Adverra Institutional Review Board (FWA 0023875) and underwent US Food and Drug Administration safety review (IND 17489). Written informed consent was obtained, including germline DNA sequencing. The trial was designed and reported by the authors, who assure the accuracy of the data. Only the authors participated in manuscript preparation. The trial was primarily supported by Stand Up to Cancer Foundation. Nivolumab was supplied by ER Squibb & Sons LLC. Aldesleukin (IL-2) was supplied by Clinigen Group, Inc. Funding to the Moffitt Cell Therapies Facility was provided by Iovance Biotherapeutics, Inc. The companies played no other role in the study or report.

**TIL product processing, selection and expansion.** The majority of collected metastases were pleural nodules or supraclavicular lymph nodes. Freshly resected patient tumors were dissected by the surgeon in a sterile back table of the operating room and adventitial tissue removed. The tumor was then placed in a sterile RPMI medium container and delivered to the Moffitt Cell Therapy Facility. Tumors were processed within 3–12 h of receipt by a cell technician within an ISO 7 cGMP certified clean room. Tumor fragments were minced into 3-mm cubes. Each tumor was cut into 48 fragments. Tumor fragments were placed individually into two separate 24-well culture plates in medium supplemented with 600 IU ml<sup>-1</sup>

of IL-2 and 10% human serum from type AB donors. Fragments were surveyed for proliferation every 2–3 days for up to 5 weeks. TILs were expanded to a new well of a 24-well plate when they became  $\geq 80\%$  confluent. TILs derived from each fragment were kept separate. Medium containing 6,000 IU ml<sup>-1</sup> IL-2 was supplemented every 3–4 days to maintain TIL growth.

T cells were screened for specificity to autologous tumors by incubation with a suspension of tumor cells and IFN- $\gamma$  quantification. For autologous reactivity testing, a portion of excess tumor was disaggregated into a single-cell suspension to create a substrate tumor for ELISA. Tumor was minced and carefully mixed in digestion medium with collagenase (type II and type IV), hyaluronidase and DNAase (Thermo Fisher Scientific). Then undigested tumor was filtered from the cell suspension to generate a single-cell suspension. Intact cells were enriched with a Ficoll-Hypaque (GE Healthcare Bio-Sciences) gradient and viable tumor cells were enumerated by trypan blue exclusion. Lymphocytes from fragment wells with the most pronounced proliferation were tested for autologous tumor reactivity by overnight co-culture with autologous tumor or allogeneic control tumor cell line in a 1:5 concentration. Allogeneic tumor cells were included as optional controls, based on predicted partial class I allele match to the patient. These included research resource identification (RRID): CVCL\_0B68, CVCL\_6789, CVCL\_8058, CVCL\_A164, CVCL\_8051, CVCL\_4632, CVCL\_8054 and CVCL\_8787.

Two 96-well plates were used per patient. A standard curve between 62 and 1,000 pg ml<sup>-1</sup> was set up for each plate. IFN- $\gamma$  within the supernatants was detected by ELISA, as shown in Extended Data Fig. 2 and analyzed using SkanIt software v.4.1. Autologous reactivity was judged based on approximately twofold or more higher IFN- $\gamma$  compared with culture medium alone. TIL pools containing reactive TILs were selected, pooled and cryopreserved for later rapid expansion protocol (REP). If insufficient or no autologously reactive TILs were identified, then additional fragments were used based on their growth rate.

Positive cultures were pooled and cryopreserved for each patient. If patients had PD on nivolumab, then TILs were thawed and expanded in CD3 antibody, irradiated allogeneic feeder cells and IL-2 over 14 d. For REP, TILs were cultured in G-Rex 100 MCS flasks and incubated at 37°C and 5% CO<sub>2</sub> at a 1:200 ratio with a layer of irradiated allogeneic donor feeder cells and IL-2 at a concentration of 3,000 IU ml<sup>-1</sup> and anti-CD3 (Ortho Biotech) at a concentration of 30 ng ml<sup>-1</sup> were added to the flasks. Flasks were incubated at 37°C and monitored for the next 7 d and split as needed to maintain TIL concentration at  $2 \times 10^6 \text{ ml}^{-1}$ . Then cells were collected, washed and concentrated to 1.01 or less. Cell viability was tested using acridine orange and propidium iodide dyes. Total live cells were counted using a Cellometer Auto 2000 (Nexcelom Bioscience). The final product was tested for sterility and then gravity infused into the patient at a rate of approximately 300 ml h<sup>-1</sup>. To characterize the final product, cells were stained with 7-AAD, CD3-FITC, CD4-PE, CD45-V500 and CD8-APC. Flow cytometry data were collected using a FACSCanto (BD Biosciences) and FlowJo Software (TreeStar). Upon collection, the TIL product underwent quality control testing and had to meet the following criteria before release for patient administration:  $\geq 45\%$  CD45<sup>+</sup> by flow cytometry,  $< 5 \text{ EU kg}^{-1}$  of endotoxin, no detectable mycoplasma, negative Gram stain,  $\geq 70\%$  viability and sterile blood culture from day -3 of REP. TILs were also assessed by flow cytometry for CD8 (mean = 57.27  $\pm$  33.77%) and CD4 (mean = 41.00  $\pm$  32.86%) composition.

**Flow cytometry of lymphocytes.** Human peripheral blood samples were collected in four heparin tubes at baseline, following nivolumab infusion and multiple time points following TIL infusion. Peripheral blood mononuclear cells (PBMCs) were collected using a Ficoll gradient and cryopreserved in 10% DMSO and FBS. Cells were thawed in medium and subsequently stained in PBS containing 5% FBS (vol/vol, FACS buffer) with CD3 BUV496, CD56 BUV563, CD4 BUV737, CD197 BV421, CD28 BV480, CD14 BV605, CD19 BV605, CD95 BV711, CD195 BV786, CD127 PE, CD194 PE-Cy7, CD45RA Alexa488, CD25 PerCP-Cy5.5, NKG2D APC, Tim-3 BV421, PD-1 BV480, CD226 BV711, CTLA4 BV786, Lag3 PE, TIGIT PE-Cy7, CD244 Alexa488, CD27 PerCP-Cy5.5 and BTLA APC (all from BD Biosciences). Dead cells were excluded using the Zombie NIR Fixable Viability kit from BioLegend, incubated at 4°C for 1 h, then washed twice with FACS buffer and finally fixed in PBS containing 1% paraformaldehyde before running flow cytometry. Cells were acquired on a BD FACSymphony A5 and data were analyzed with FlowJo v.10.0 software. All cell gates were drawn uniformly for analysis across patients and time points, with gating strategy provided in Supplementary Appendix 2. Plots of *t*-SNE were generated by FlowJo v.10.6.1 according to the expression of CD45RA, CCR7, CD28 and CD95. Different memory T cell subsets were shown using separate colors.

**Polyfunctional strength index.** PSI measures the ability of single CD3<sup>+</sup> cells to secrete multiple different cytokines after stimulation<sup>29</sup>. CD8<sup>+</sup> T cells were sorted from TILs and peripheral blood and stimulated with CD28 and CD3 antibody as previously described<sup>45</sup>. Testing was performed using the Isoplex IsoCode chip using the 12 human cytokine single-cell proteome panel. For PSI, data from empty chambers are used to measure the background level for each protein. These data were used to generate protein abundance histograms, which are fitted by normal distributions and nonparametric methods, judged by goodness of fit. The mean of the histogram, identified by the best fit, is used as the background

level. Single-cell data were then normalized by subtracting this background, so that different samples can be compared. The single-cell data were then fitted by finite mixture models and the gate that separates the cytokine-producing and noncytokine-producing cells was identified. Pre- and post- infusion time points were compared using a mixed-effects model (REML) with stacked matching with Geisser–Greenhouse correction, in an exploratory comparison. Multiplicity adjusted *P* value was performed using Dunnett's control.

**Generation of autologous dendritic cells.** The plastic adherence method was used to generate monocyte-derived DCs. Autologous PBMCs or apheresis samples were thawed and resuspended at  $2\text{--}5 \times 10^6 \text{ ml}^{-1}$  with AIM-V medium (Life Technologies). The cells were incubated in a tissue culture flask of an appropriate size at  $37^\circ\text{C}$ , 5%  $\text{CO}_2$ . After 90 min, nonadherent cells were collected and flasks were washed with AIM-V medium twice with an interval of 60 min, after which DC medium was added. DC medium was made from RPMI 1640 containing 5% human serum (Sigma),  $100 \text{ U ml}^{-1}$  penicillin and  $100 \text{ U ml}^{-1}$  streptomycin, 2 mM L-glutamine (media supplements were from Life Technologies),  $800 \text{ IU ml}^{-1}$  GM-CSF and  $800 \text{ U ml}^{-1}$  IL-4 (cytokines from Peprotech). On day 3, fresh DC medium was supplemented. DCs were collected on day 5–7 and frozen in 10% DMSO for co-culture experiments.

**Screening T cells for reactivity to antigens using the ELISpot assay.** Both effector T cells and DCs were pre-thawed 24 h before co-culture in IL-2 free medium. In the ELISpot assay, PVDF membrane plates (Millipore, MAIPSWU10) were pre-activated with  $50 \mu\text{l}$  70% ethanol per well for 2 min and washed three times with PBS. Then  $50 \mu\text{l}$  purified IFN- $\gamma$  capture antibody (Mabtech, clone, 1-D1K) was added per well for incubation at  $4^\circ\text{C}$  overnight. Before co-culture, wells were washed three times with PBS and incubated with  $100 \mu\text{l}$  AIM-V medium at room temperature for 1 h. In co-culture, when using TILs as effector T cells,  $1 \times 10^4$  to  $3 \times 10^4$  T cells were placed per well in a 96-well flat bottom plate. When T cells isolated from apheresis samples (4 weeks after TIL infusion) were used as effector cells,  $1 \times 10^5$  cells were used per well in a 96-well flat bottom plate. Effector T cells were co-cultured with  $5 \times 10^3$ – $1 \times 10^4$  DCs loading 1– $10 \mu\text{g ml}^{-1}$  tumor antigen peptides. Cytomegalovirus, Epstein–Barr, or influenza (CEF) viral peptides and/or plate-bound OKT3 ( $1 \mu\text{g ml}^{-1}$ ) were used as positive controls. Effector T cells only and/or effector T cells co-cultured with unloaded DCs were used as negative controls.

After 24 h of co-culture, the plate was washed 6 $\times$  with PBS plus 0.05% Tween-20 and then incubated with  $100 \mu\text{l}$  per well of  $0.22 \mu\text{m}$  filtered  $1 \mu\text{g ml}^{-1}$  biotinylated anti-IFN- $\gamma$  detection antibody (Mabtech, clone, 7-B6-1) for 2 h. Another 4 $\times$  wash with PBS-T was performed and  $100 \mu\text{l}$  per well of streptavidin-ALP (Mabtech, diluted 1:1,000) was added for a 1-h incubation. The plate was washed 6 $\times$  with PBS and developed with  $100 \mu\text{l}$  per well of  $0.45 \mu\text{m}$  filtered BCIP/NBT substrate solution (KPL) for 10 min. Finally, the plate was washed thoroughly with cold tap water and then scanned and auto-counted using an ImmunoSpot ELISpot plate reader (Cellular Technologies).

**Identification of tumor antigen-specific TCR clonotypes (FEST).** Our protocol to identify tumor antigen-specific TCR clonotypes followed the published MANIFEST assay<sup>46</sup> with modifications. Apheresis samples (4 weeks after TIL infusion) were thawed and T cells were isolated using EasySep Human T cell Enrichment Kit (Stemcell Technologies). Then T cells were washed and resuspended at  $2 \times 10^6 \text{ ml}^{-1}$  in AIM-V medium. DCs were thawed and resuspended at  $5 \times 10^4 \text{ ml}^{-1}$  in AIM-V medium. After identifying T cell-recognized tumor antigens,  $125 \mu\text{l}$  T cells were co-cultured with  $125 \mu\text{l}$  DCs in a 96-well round-bottom plate and tumor antigen proteins/peptides were added at 1– $10 \mu\text{g ml}^{-1}$ . On day 3, supernatants were half replaced with fresh AIM-V medium containing  $100 \text{ IU ml}^{-1}$  IL-2,  $50 \text{ ng ml}^{-1}$  IL-7 and  $50 \text{ ng ml}^{-1}$  IL-15. On day 7, supernatants were half replaced with fresh AIM-V medium containing  $200 \text{ IU ml}^{-1}$  IL-2,  $50 \text{ ng ml}^{-1}$  IL-7 and  $50 \text{ ng ml}^{-1}$  IL-15. Cell cultures were collected on day 10 for DNA extraction (QIAGEN) and further TCR-V $\beta$  sequencing. Analysis of TCR-seq data to determine tumor antigen-specific expansion of TCR clonotypes was performed using the online tool at <http://www.stat-apps onc.jhmi.edu/FEST><sup>46</sup>.

The absolute number of T cell clonotypes in peripheral blood was calculated by using the absolute lymphocyte count derived from automated cell differential provided by the medical laboratory, multiplied by the percentage of CD3<sup>+</sup> gated of all lymphocytes by flow cytometry, multiplied by the frequency of this specific clone as a proportion of all productive rearrangements derived from immunoSEQ TRV- $\beta$  DNA sequencing of that sample.

**Analysis of tumor markers.** Resected baseline tumors were stained for PD-L1 using 22C3 pharmDx immunohistochemistry antibody and scored using TPS by a trained pathologist. TMB was originally estimated using targeted exome sequencing from Foundation Medicine. After completion of WES, it was calculated by dividing the total number of nonsynonymous mutations by the total length of exome regions. All tumor marker inferences were defined as exploratory in the study protocol.

**Nucleic acid extraction.** Portions of the same tumor resected for TILs were snap-frozen in liquid nitrogen and stored at  $-80^\circ\text{C}$ . In batches, tumor regions of interest were selected based on H&E sections using laser-capture macrodissection

(LCMD) and pulverized into aliquots of 15 mg. Aliquots were extracted for RNA and DNA using Allprep kits (QIAGEN). DNA and RNA was quantified using Invitrogen Qubit Fluorometer, purity assessed using Thermo Scientific NanoDrop and integrity assessed with Agilent 4200 TapeStation system. Mononuclear cells were isolated from peripheral blood collected in EDTA tubes, using a Ficoll gradient. Cell pellets were snap-frozen and later DNA was extracted in water using mini-prep kit (QIAGEN). Quality metrics were assessed as described above.

**Whole-exome sequencing.** WES was performed to identify somatic mutations in DNA extracted from pre-treatment tumor tissue. Two hundred nanograms of DNA was used as input into the Agilent SureSelect XT Clinical Research Exome kit, which includes the exon targets of Agilent's v5 whole-exome kit, with increased coverage at 5,000 disease-associated targets. Briefly, for each tumor DNA sample and germline DNA sample, a genomic DNA library was constructed according to the manufacturer's protocol and the size and quality of the library was evaluated using the Agilent BioAnalyzer. An equimolar amount of library DNA was used for a whole-exome enrichment using the Agilent capture baits and after quantitative PCR library quantitation and quality control analysis on the BioAnalyzer, 75-base paired-end sequences were generated using v2 chemistry on an Illumina NextSeq 500 sequencer.

HLA class I and II locus sequencing was performed in the Moffitt HLA laboratory (ASHI accreditation 07-3-FL-18-1). DNA from nucleated peripheral blood cells underwent quality control using Nanodrop followed by next generation sequencing using the MIA FORA FLEX HLA Typing kit (Immucor). A confirmatory sequence-specific oligonucleotide (SSO) DNA typing (LABType, One Lambda) was performed to resolve ambiguous alleles.

**Transcriptome sequencing.** RNA-sequencing libraries were prepared from RNA extracted from pre-treatment tumor tissue using the NuGen FFPE RNA-Seq Multiplex System (Tecan US). Briefly, 50 ng of DNase-treated RNA was used to generate complementary DNA and a strand-specific library following the manufacturer's protocol. Library molecules containing ribosomal RNA sequences were depleted using the NuGen AnyDeplete probe-based enzymatic process. Final libraries were assessed for quality on the Agilent TapeStation (Agilent Technologies) and quantitative PCR with reverse transcription (RT-PCR) for library quantification was performed using the Kapa Library Quantification kit (Roche Sequencing). Libraries were sequenced on the Illumina NextSeq 500 sequencer with a 75-base paired-end run to generate 80–100 million read pairs per sample.

**T cell repertoire sequencing.** T cell receptor repertoire analysis was performed using Adaptive Biotechnologies immunoSEQ v3 assay, which employs bias-controlled multiplex PCR amplification and high-throughput sequencing to target rearranged T cell receptor genes. The manufacturer's protocol was followed to utilize the immunoSEQ hsTCRB kit to amplify the complementarity-determining region 3 (CDR3) locus from genomic DNA extracted from sorted T cells or tissue. Following confirmation of amplification and a successful final library preparation, sequencing was performed on the Illumina NextSeq 500 to a depth of 2 million pairs of sequencing reads per sample for survey-level analysis, or 5–6 million pairs per sample for deep-level analysis. The data were then analyzed using the Adaptive Biotechnologies immunoSEQ Analyzer software, which identifies and counts the V, D and J genes, filters nonproductive sequences and reports and tracks T cell clonality.

**Proteomics.** Tissue samples were pulverized and denaturing buffer was used to extract the proteins, followed by protein reduction, alkylation and trypsin digestion. The tryptic peptides were acidified and desalted with C18 cartridge. After lyophilization, peptides were fractionated off-line with basic pH reversed-phase HPLC and 24 concatenated fractions were collected. LC-MS/MS analysis of each fraction was performed with a nanoflow ultra-high performance liquid chromatograph (RSLC) coupled to an electrospray bench top orbitrap mass spectrometer (Q-Exactive plus, Thermo). The result was analyzed with MaxQuant software for protein identification and label-free quantitation<sup>47</sup>.

**Identification of somatic mutations.** Somatic mutations were identified from WES reads and aligned to the reference human genome (hg19) with the Burrows–Wheeler Aligner (BWA)<sup>48</sup>. Insertion/deletion realignment and quality score recalibration were performed with the Genome Analysis ToolKit<sup>49</sup>. Tumor-specific mutations were identified with Strelka<sup>50</sup> and MuTect<sup>51</sup> and were annotated to determine genic context, including nonsynonymous, missense, splicing calls, using ANNOVAR<sup>52</sup>. Only somatic mutations predicted by both algorithms were included for subsequent neoantigen prediction. Additional contextual information was incorporated, including allele frequency was derived from available resources including 1000 Genomes, the NHLBI Exome Sequence Project and the Exome Aggregation Consortium<sup>53</sup>, in silico function impact predictions and observed impacts from databases including ClinVar (<http://www.ncbi.nlm.nih.gov/clinvar/>) and the Collection of Somatic Mutations in Cancer.

**Gene expression and fusion detection.** Sequence reads were aligned to the human reference genome in a splice-aware fashion using STAR<sup>54</sup>, allowing for

accurate alignments of sequences across introns. Aligned sequences were assigned to exons using the HTseq package<sup>55</sup>. DESeq2 was used for normalization of gene expression<sup>56</sup>. Aberrant cancer testis antigen (MAGE) expression was identified based on gene expression level and verified using the sum of peptide intensities for the corresponding fasta protein proteomic sequencing described above. Gene fusions were identified from RNA-seq data using FusionCatcher (<https://doi.org/10.1101/011650v1>).

**Neoantigen prediction and prioritization.** Neoantigens will be identified by extracting altered peptides from mutation data with ANNOVAR or directly from FusionCatcher results and then predicting MHC binding against patient-specific HLA type using NetMHC<sup>57</sup>, NetMHCpan<sup>58</sup> and NetMHCIIpan<sup>58</sup> as implemented by the Immune Epitope Database<sup>59</sup>. HLA types were derived from clinical HLA laboratory sequencing data. Neoantigens were prioritized by a combination of predicted MHC binding affinity, variant allele frequency, RNA expression of genes where the mutation is potentially located and evidence of reads carrying the mutated base.

**Statistical analysis.** Adverse events were continuously monitored. Acceptable safety was prospectively defined as a dose-limiting toxicity rate of 17% or less, using a Pocock-type stopping boundary with continuous monitoring<sup>60</sup>. Dose-limiting toxicity was defined as grade  $\geq 4$  toxicity with attribution to ACT, detailed with sample size justification in the **Supplementary Protocol**. Baseline tumor measurements were defined on week  $-1$  CT before TIL treatment, with subsequent assessment every 6 weeks. Overall survival was calculated using the Kaplan–Meier method and 95% confidence interval was included for medians and curves. Pathological, genomic and functional immunologic testing was performed and analyzed as described in the **Supplementary Protocol**. Reported *P* values were two-sided with a significance of 0.05, unless otherwise noted. Normality was not assumed and nonparametric tests were performed where applicable. For functional expansion of specific T cells (FEST) analysis, a threshold *P* value of 0.05 was adjusted by Benjamini–Hochberg procedure to control for multiple comparisons, as previously published<sup>46</sup>. Data were analyzed in R v.3.6.3 (2020-02-29), using Windows 10 x64 operating system, ming w32, user interface ‘RTerm’ language English–United States and Prism 9.0 (22 October 2020).

**Reporting Summary.** Further information on research design is available in the Nature Research Reporting Summary linked to this article.

## Data availability

TRV- $\beta$  sequencing of tumor and peripheral T cells as the project ‘TIL trial for NSCLC’ are available in the ImmuneACCESS free public database at <https://clients.adaptivebiotech.com/immuneaccess>. Tumor WES and RNA-seq raw data files are available on the public National Institutes of Health (NIH) dbGaP data browser ([https://www.ncbi.nlm.nih.gov/projects/gap/gapcgi-bin/preview1.cgi?GAP\\_phs\\_code=Ug9rhvZ3dGC4uQSh](https://www.ncbi.nlm.nih.gov/projects/gap/gapcgi-bin/preview1.cgi?GAP_phs_code=Ug9rhvZ3dGC4uQSh); accession code phs002486.v1.p1). Raw data on expression, allelic frequency and predicted MHC affinity for all identified neoantigens are provided in the Excel spreadsheet in Supplementary Table 4. The study protocol is uploaded as a supplementary file. In the event that source data are not inferred from specified tables/figures, they are available upon request in a comma-delimited format from the study authors.

## References

- Andersen, R. et al. Long-lasting complete responses in patients with metastatic melanoma after adoptive cell therapy with tumor-infiltrating lymphocytes and an attenuated IL2 regimen. *Clin. Cancer Res.* **22**, 3734–3745 (2016).
- Xue, Q. et al. Single-cell multiplexed cytokine profiling of CD19 CAR-T cells reveals a diverse landscape of polyfunctional antigen-specific response. *J. Immunother. Cancer* **5**, 85 (2017).
- Danilova, L. et al. The mutation-associated neoantigen functional expansion of specific T cells (MANAFEST) assay: a sensitive platform for monitoring antitumor immunity. *Cancer Immunol. Res.* **6**, 888–899 (2018).
- Cox, J. & Mann, M. MaxQuant enables high peptide identification rates, individualized ppb-range mass accuracies and proteome-wide protein quantification. *Nat. Biotechnol.* **26**, 1367–1372 (2008).
- Li, H. & Durbin, R. Fast and accurate short read alignment with Burrows–Wheeler transform. *Bioinformatics* **25**, 1754–1760 (2009).
- DePristo, M. A. et al. A framework for variation discovery and genotyping using next-generation DNA sequencing data. *Nat. Genet.* **43**, 491 (2011).
- Saunders, C. T. et al. Strelka: accurate somatic small-variant calling from sequenced tumor–normal sample pairs. *Bioinformatics* **28**, 1811–1817 (2012).
- Cibulskis, K. et al. Sensitive detection of somatic point mutations in impure and heterogeneous cancer samples. *Nat. Biotechnol.* **31**, 213–219 (2013).
- Wang, K., Li, M. & Hakonarson, H. ANNOVAR: functional annotation of genetic variants from high-throughput sequencing data. *Nucleic Acids Res.* **38**, e164–e164 (2010).

- Lek, M. et al. Analysis of protein-coding genetic variation in 60,706 humans. *Nature* **536**, 285–291 (2016).
- Dobin, A. et al. STAR: ultrafast universal RNA-seq aligner. *Bioinformatics* **29**, 15–21 (2013).
- Anders, S., Pyl, P. T. & Huber, W. HTSeq: a Python framework to work with high-throughput sequencing data. *Bioinformatics* **31**, 166–169 (2015).
- Anders, S. & Huber, W. Differential expression analysis for sequence count data. *Genome Biol.* <https://doi.org/10.1186/gb-2010-11-10-r106> (2010).
- Nielsen, M. et al. Reliable prediction of T-cell epitopes using neural networks with novel sequence representations. *Protein Sci.* **12**, 1007–1017 (2003).
- Reynisson, B. et al. Improved prediction of MHC II antigen presentation through integration and motif deconvolution of mass spectrometry MHC eluted ligand data. *J. Proteome Res.* <https://doi.org/10.1021/acs.jproteome.9b00874> (2020).
- Vita, R. et al. The immune epitope database (IEDB): 2018 update. *Nucleic Acids Res.* **47**, D339–D343 (2019).
- Ivanova, A., Qaqish, B. F. & Schell, M. J. Continuous toxicity monitoring in phase II trials in oncology. *Biometrics* **61**, 540–545 (2005).

## Acknowledgements

This work was supported by a Catalyst Award Clinical Trial grant through the Stand Up to Cancer Foundation (SU2C-AACR-CT04-17; to E.B.H., S.J.A.); Barbara Bauer Prelude to a Cure Foundation grant to B.C.C.; ER Squibb for nivolumab supply; Iovance Biotherapeutics as a research grant, Clinigen for aldesleukin supply, an NCI Cancer Center Support Grant (P30-CA076292; to E.B.H.) and 2018 Young Investigator award from Adaptive Biotechnologies to B.C.C. Stand Up 2 Cancer is a program of the Entertainment Industry Foundation administered by the American Association for Cancer Research. We thank the patients and their families who participated in this research; members of the Moffitt Cell Therapies Facility, including L. Kelley and C. Cox for cell manufacturing; C. Yang and T. Mesa at the Moffitt Molecular Genomics Facility, M. Wloch, N. Smith and K. Fahrner at the Moffitt Tissue Core and P. Cano at the Moffitt Histocompatibility Leukocyte Antigen laboratory; T. Boyle and G. Zhang for assistance with clinical specimens; C. Ulge for grant administration; M. Avedon for translational project management; and other members of our clinical and laboratory research teams. Cell sorting for this project was performed on instruments in the Moffitt Flow Cytometry Core. Sequencing was performed by the Moffitt Molecular Genomics and Proteomics & Metabolomics Core Facilities (supported in part by NCI Cancer Center Support Grant P30-CA076292). Clinical care and trial coordination was provided by the Moffitt Immune and Cellular Therapies department. We thank B. Banbury for assistance with the graphs of T cell clonotypes.

## Author contributions

The trial protocol was designed and written by the authors (B.C.C., A.A.S. and S.J.A.). S.A.A. and F.J.K. obtained grant funding. L.B.M. and W.C. coordinated the trial initiation and study procedures. Z.J.T. and D.-T.C. analyzed the clinical data and performed statistical analysis. E.B., B.C.C. and S.J.A. interpreted clinical data. C.W. and D.R.N. performed immunologic assays. S.K. and C.W. performed and supervised flow cytometry. J.K.T. and J.Y. performed and interpreted bioinformatics analyses. J.T.S. performed immunohistochemical staining scoring. Work related to TIL production was conducted and supervised by A.M.L. RNA and DNA sequencing preparations were supervised by B.C.C. and C.W. Genomic sequencing was performed and supervised by S.J.Y. Proteomic sequencing was performed and supervised by J.M.K. and B.Y. T.T., A.N.S., A.A.C., S.J.A. and B.C.C. informed patients and were responsible for patient care. E.M.T. and J.E.M. performed TIL surgery. S.P.T., E.B.H., S.J.A. and J.C.G. provided scientific input during protocol design and interpretation of the study. The manuscript was written by B.C.C. and C.W., together with all co-authors, who vouch for the accuracy of the data reported and adherence to the protocol. All authors edited and approved the manuscript.

## Competing interests

Moffitt Cancer Center (Principal Investigator B.C.C.) was the sponsor of the trial. The trial was primarily supported by Stand Up to Cancer Foundation through the AACR Catalyst grant mechanism. Nivolumab was supplied by ER Squibb & Sons. Aldesleukin (IL-2) was supplied by Clinigen Group. Funding to the Moffitt Cell Therapies Facility was provided by Iovance Biotherapeutics. The companies played no other role in the study or report. B.C.C. has received speaking fees from AstraZeneca, ARIAD Pharmaceuticals and Hoffmann–La Roche and consultant fees from Xilio, Achilles, ER Squibb, Hoffmann–La Roche, AstraZeneca, AbbVie, KSQ Therapeutics, GlaxoSmithKline, Gilead Sciences, Celgene. B.C.C. has received research funding from NeoGenomics Laboratories and Adaptive Biotechnologies and has a patent application (WO2020263919A1). A.A.C. has received speaking fees from Genentech, Merck, Celgene and Takeda; consultant fees from Amgen, Jazz, AstraZeneca, Pfizer, Novartis, AbbVie and BMS; and research funding from AstraZeneca, Novartis and BMS, outside the submitted work. J.R.C.G. has received consultant fees from Leidos, consultant and nonfinancial support from Anixa Biosciences; consultant fees and nonfinancial support from Compass Therapeutics; and has a patent (WO2020033923A1) pending. E.B.B. has received consultant fees from Amgen and Janssen, outside the submitted work. S.K. reports nonfinancial and research financial support from BMS and AstraZeneca.

A.M.L. received financial support from Iovance Biotherapeutics. J.E.M. reports laboratory research support from Iovance Biotherapeutics for research outside the submitted work and a patent (62668246) licensed to Iovance Biotherapeutics. S.A.P.T. reports grants from Swim Across America Foundation, V Foundation, American Cancer Society Research Scholar Grant, State of Florida Bankhead-Coley Grant, Iovance Biotherapeutics, Intellia Therapeutics, Myst Therapeutics, NIH-NCI (grant nos. U54 CA193489-01A1, CA241559, U01 CA244100-01, R01 CA239219-01A1) and Provectus Biopharmaceuticals, outside the submitted work. In addition, S.A.P.T. has a patent (61/973,006 61/978,112) with royalties paid to Iovance Biotherapeutics and a patent immunotherapy targeted to tumors expressing receptors with royalties paid to Tuhura Biopharma. A.N.S. received nonfinancial support and research grants from Daiichi Sankyo, Novartis, Mersana, Genmab and Eli Lilly, outside the submitted work. A.A.S. reports grants from NCI K23, Ocala Royal Dames and Swim Across America Foundation; personal fees from Guidepoint and Gerson Lehrman Group; and consultant fees from Defined Health, Iovance Biotherapeutics, Physicians' Educational Resource and Medscape, outside the submitted work. In addition, A.A.S. has a patent for Compositions and Methods for Improving Tumor-infiltrating Lymphocytes for Adoptive Cell Therapy (61/973,002) with royalties paid to Iovance Biotherapeutics, a patent for a Rapid Method for Culture of Tumor-infiltrating Lymphocytes from Core Needle Biopsies of Solid Tumors and a patent for Tumor-infiltrating Lymphocytes and Stapled Peptoid Peptide Hybrid Peptidomimetics (16/157,174). J.K.T. has grant support through P30-CA76292

and a patent pending for a Large Data Set Negative Information Storage Model. C.W. has a patent application filed for Generation of T Cell Receptors (TCRs) that React to Neoantigens. S.J.A. has received advisor fees from Achilles, Amgen, AstraZeneca, ER Squibb, Caris Life Sciences, Celsius Therapeutics, G1 Therapeutics, GlaxoSmithKline, Mengden, Merck & Co., Nektar Therapeutics, RAPT Therapeutics, Venn Therapeutics, Glympse, EMD Serano and Samyang Biopharm USA; and research funding from Cellular Biomedicine Group. The remaining authors declare no competing interests.

### Additional information

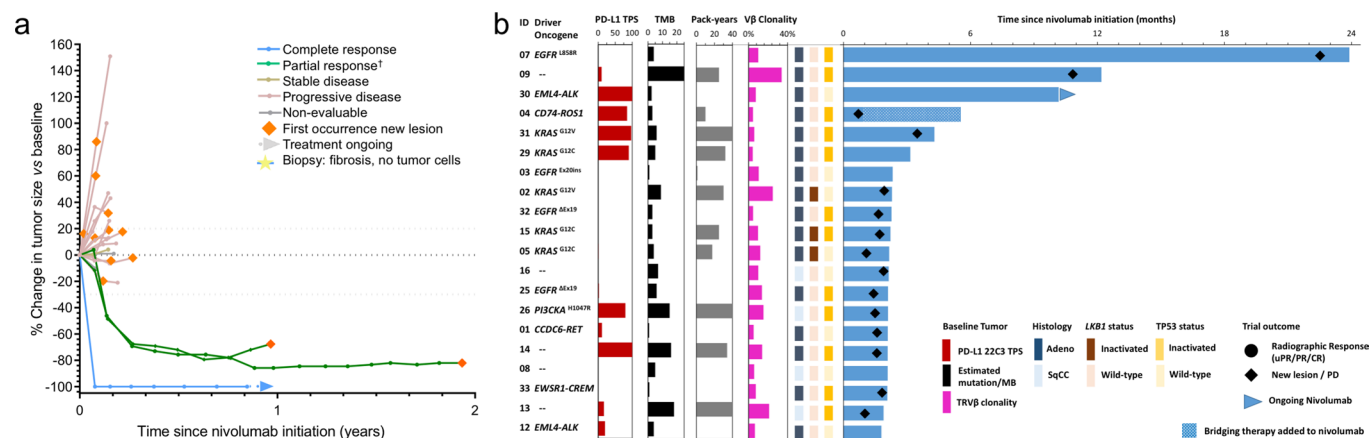
**Extended data** is available for this paper at <https://doi.org/10.1038/s41591-021-01462-y>.

**Supplementary information** The online version contains supplementary material available at <https://doi.org/10.1038/s41591-021-01462-y>.

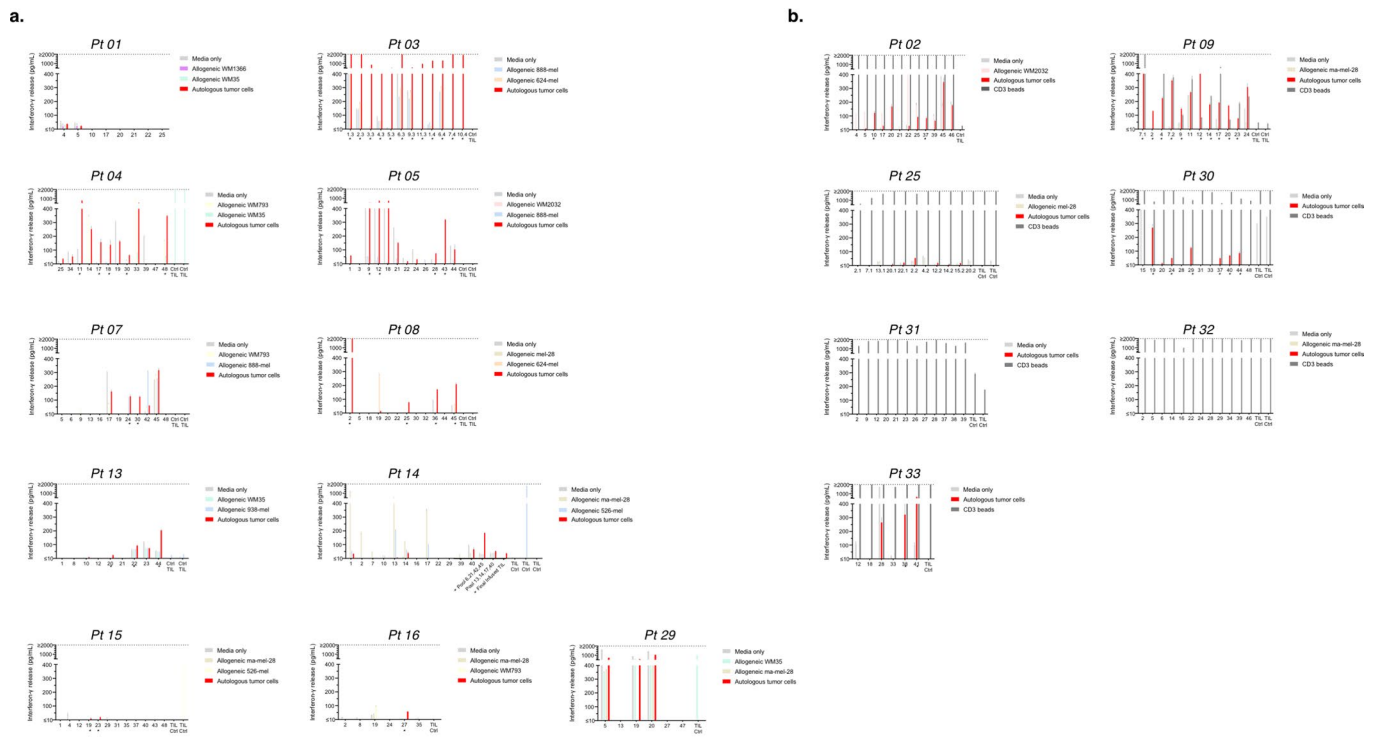
**Correspondence and requests for materials** should be addressed to B.C.C.

**Peer review information** *Nature Medicine* thanks Pia Kvistborg, Solange Peters, Qian Wu and the other, anonymous, reviewer(s) for their contribution to the peer review of this work. Javier Carmona was the primary editor on this article and managed its editorial process and peer review in collaboration with the rest of the editorial team.

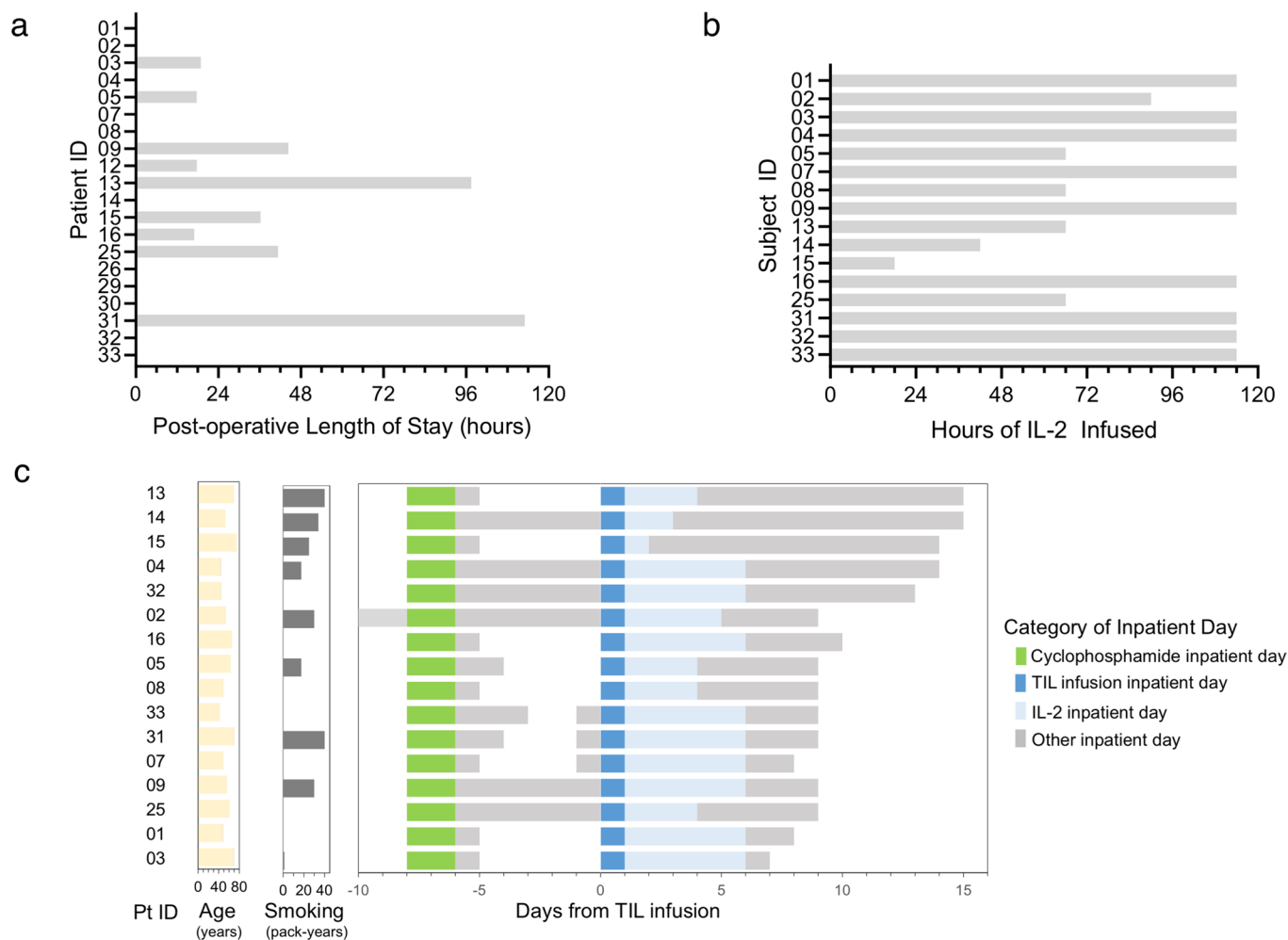
**Reprints and permissions information** is available at [www.nature.com/reprints](http://www.nature.com/reprints).



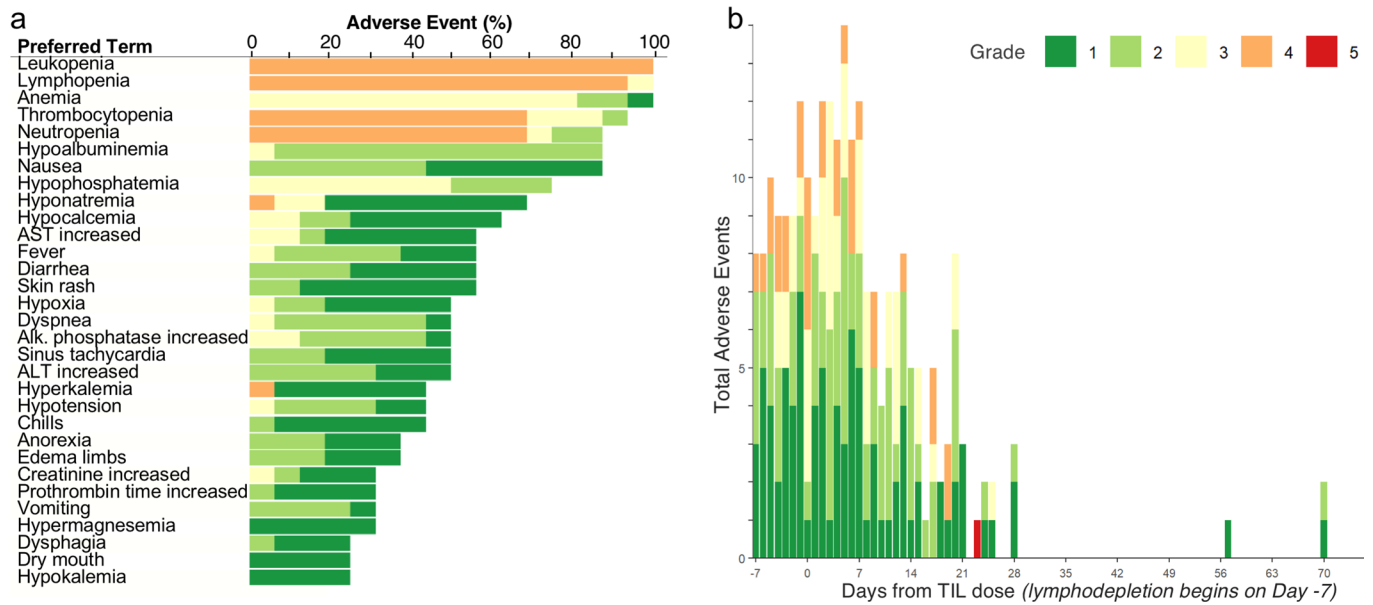
**Extended Data Fig. 1 | Clinical follow-up after initial nivolumab.** **a**, Sum of tumor diameters per RECIST v1.1 over time measured by serial CT scan. Patients with evidence of tumor enlargement or new lesions within 10 weeks of initial nivolumab were treated with TIL infusion. All enrolled patients ( $n=20$ ) are included. **b**, Clinical follow-up of patients after initial nivolumab with clinicopathologic features in a Swimmer's plot. Pt 04 received bridging crizotinib due to rapid progression on nivolumab. Abbreviations: TPS denotes tumor proportion score using 22C3 PD-L1 antibody. TMB; estimated tumor mutation burden based upon exome sequencing. mut/MB mutations per mega-base. 'Ex' denotes exon, and 'Δ' denotes mutation conferring exon deletion. Smoking pack-years represents self-reported cigarette packs per day multiplied by total years.



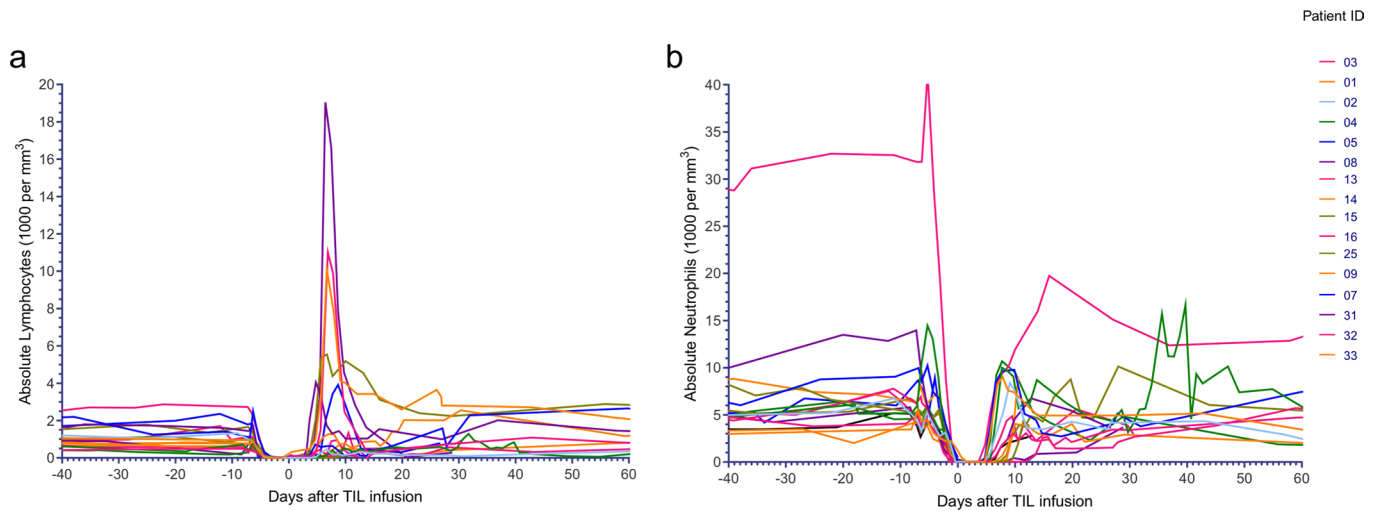
**Extended Data Fig. 2 | Autologous reactivity screening of TIL cultured from individual tumor fragments in combination with baseline tumor cell suspensions.** Shown are the interferon- $\gamma$  enzyme-linked immunosorbent assays conducted without (a) and with (b) CD3 bead positive controls. Each graph is labeled with the trial patient ID. The x-axis represents the TIL fragment selected for testing. Each fragment number represents an autologous T cell line generated from a unique tumor morsel cultured in IL-2 and media between 3 to 5 weeks. Each culture is labelled by its original fragment identification number, from 48 total per patient. Post-decimal numerals indicate the tumor number, if multiple tumor sites were harvested for the same patient. An asterisk denotes whether the fragment was deemed autologously reactive. Shown is the mean  $\pm$  SEM of triplicate wells from a single ELISA experiment. Each bar denotes one biologically independent culture sample ( $n=1$ ). ' $\leq 10'$ ' denotes a sample with absorbance reading below the lowest point of the standard curve performed for each assay. 'TIL Ctrl' denotes a TIL culture derived from an unrelated patient to serve as a positive control for the CD3 beads and a negative control for autologous substrate. Allogeneic cancer cell lines were selected as an optional control based on partial HLA class I allele compatibility with the patient. Patient ID 12 did not have sufficient TIL growth for manufacture, and ID 26 did not have sufficient tumor for autologous reactivity testing.



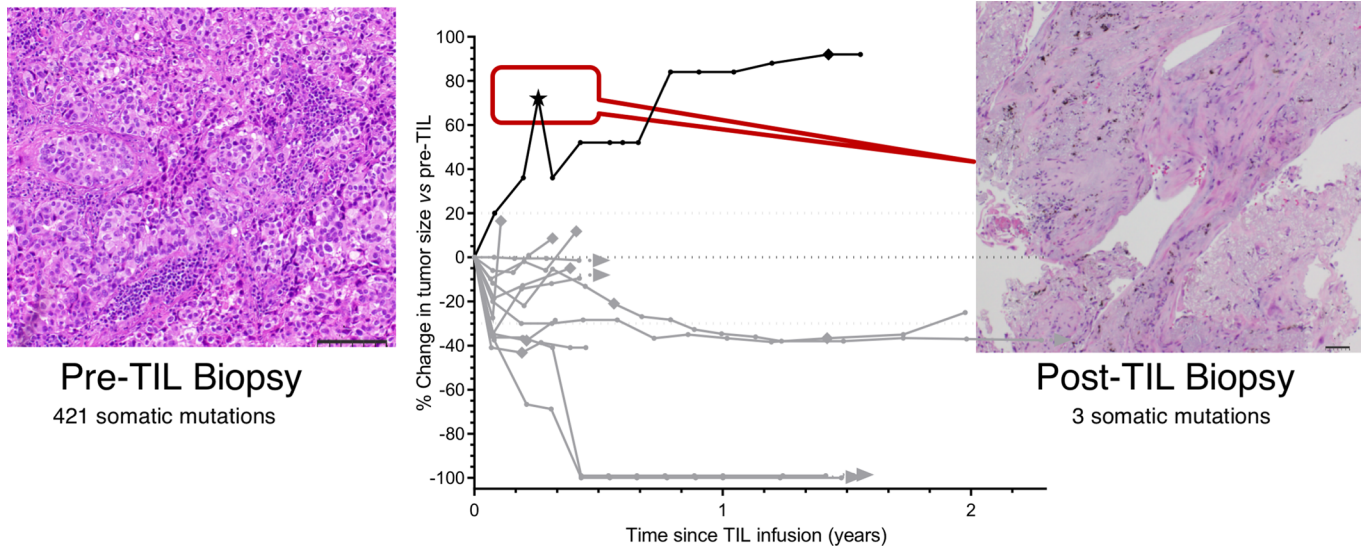
**Extended Data Fig. 3 | Feasibility of TIL harvest and intermediate-dose interleukin-2 infusion for all patients.** **a**, Total hours of length of stay (LOS) for inpatient admissions after TIL harvest surgery. Two patients had postoperative air-leak requiring multiple days of inpatient observation. All enrolled patients ( $n=20$ ) are included. **b**, The total duration of infusional IL-2 for all 16 patients after TIL treatment. Patients received TIL infusion on Day 0, followed by continuous IL-2 infusion beginning 12 hours later at a dose of 18 million international units (MIU) per m<sup>2</sup> over 6, then 12, and then 24 hours followed by 4.5 MIU/m<sup>2</sup> over 24 hours for 3 consecutive days. **c**, Total inpatient length of stay for all patients. Some patients were discharged to outpatient between cyclophosphamide admission and TIL admission.



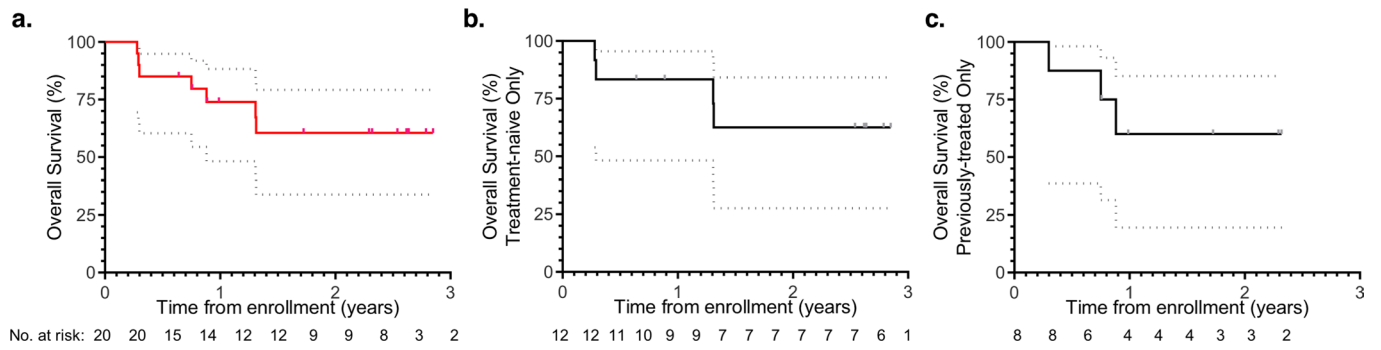
**Extended Data Fig. 4 | Treatment-emergent adverse events reported with cyclophosphamide, fludarabine, TIL, and IL-2.** **a**, Adverse events grouped by National Cancer Institute preferred term occurring in 20% or more of patients attributable to cyclophosphamide, fludarabine, TIL, or IL-2. All TIL treated patients ( $n=16$ ) are included. **b**, All adverse events grouped by date of onset within 3 months of TIL. Patients with multiple events for a given term are counted once, using the maximum grade under each preferred term. Abbreviations: AE denotes adverse events; AST denotes aspartate aminotransferase; ALT denotes alanine aminotransferase; IL-2, interleukin-2.



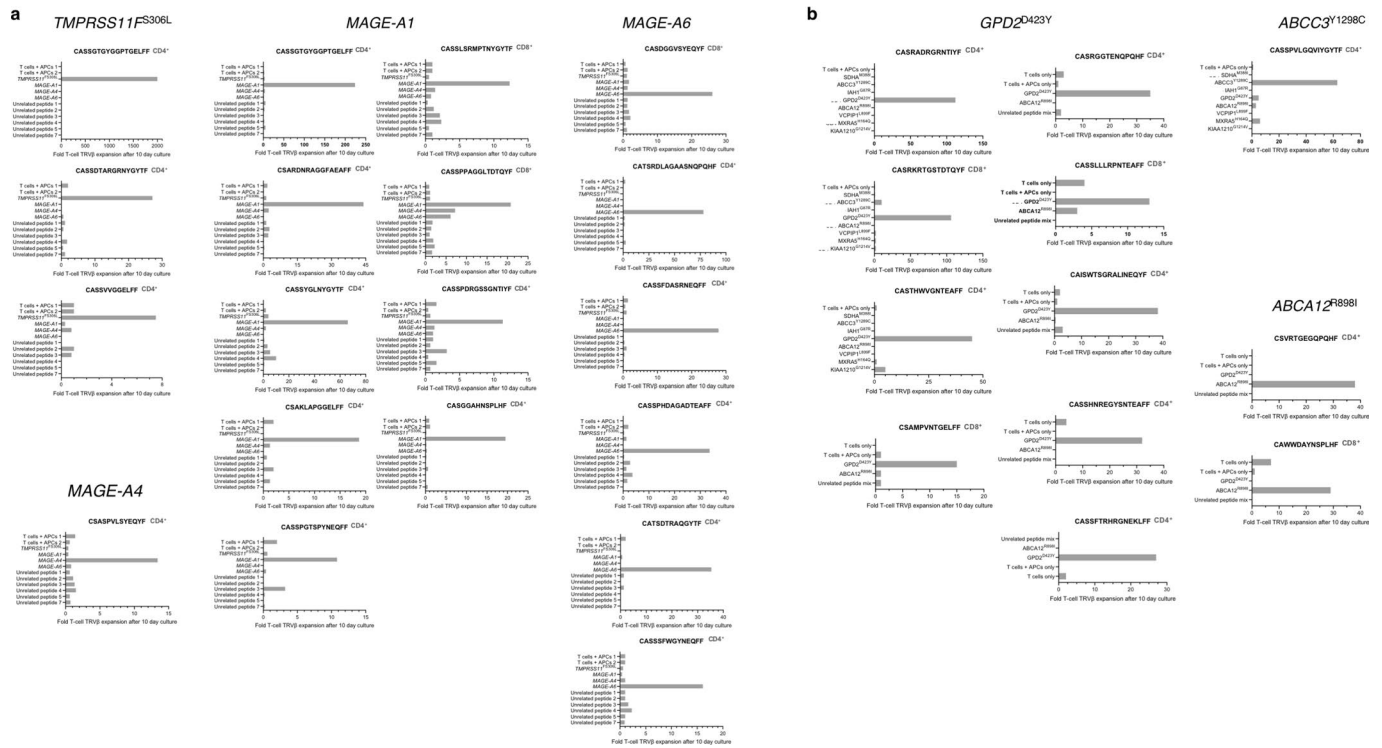
**Extended Data Fig. 5 | Change in lymphocytes and neutrophils with lymphodepletion, TIL, and IL2. a**, Initial peak followed by recovery of peripheral blood absolute lymphocyte count. **b**, peripheral blood absolute neutrophil count recovered by median of 7.5 days (range 4.7 - 20.6). Shown is absolute cell count (1000 cells per mm<sup>3</sup>). TIL infusion is 'Day 0'. All TIL treated patients are shown ( $n = 16$ ).



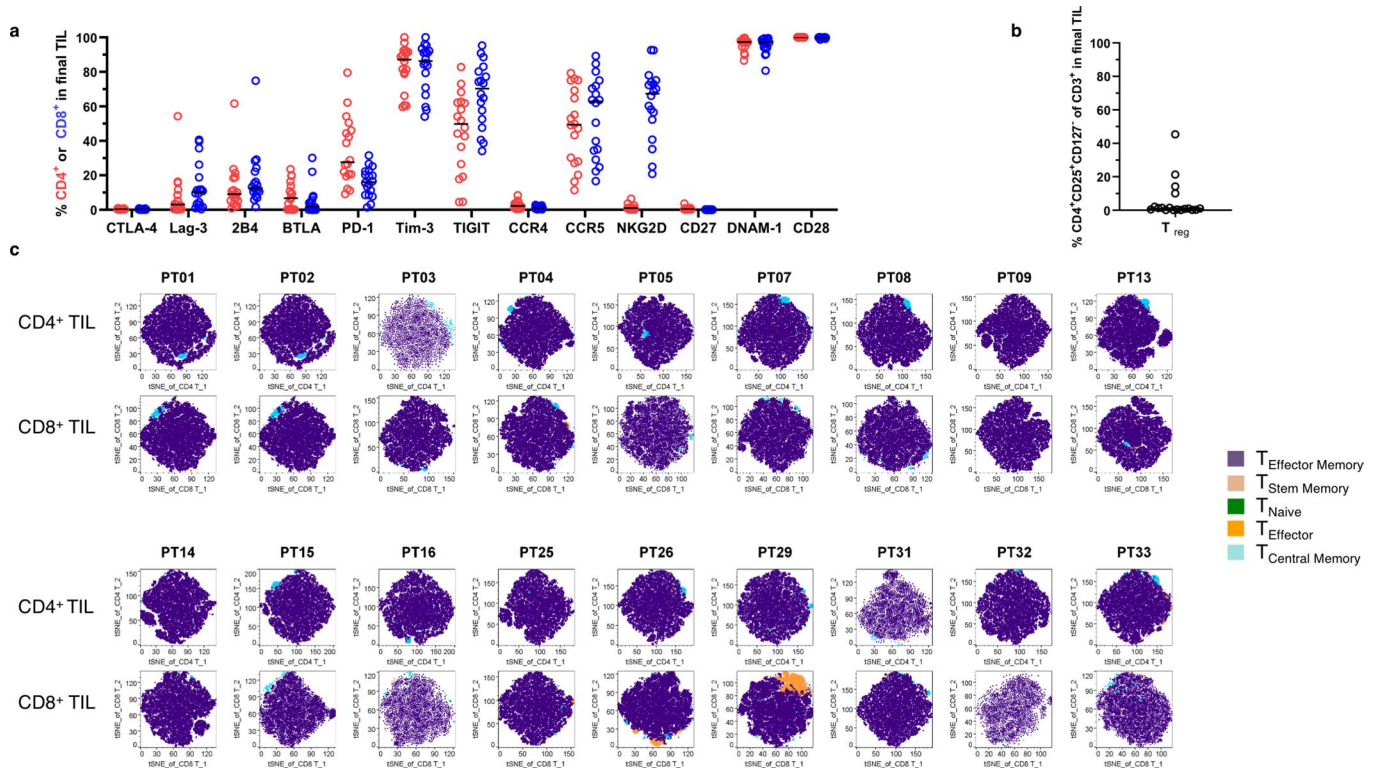
**Extended Data Fig. 6 | Radiographic enlargement of a target lesion in patient 14.** Patient had biopsy-proven lung adenocarcinoma biopsy proven from a lymph node metastasis and pleural mass. She had increase in her only target lesion pleural metastasis post-TIL and biopsy revealed fibrosis. Whole exome sequencing conducted on the original tumor showed over four hundred somatic mutations. Only 3 mutations could be detected in the post-TIL biopsy despite 200x depth of sequencing. She had new metastases appear 1.4 years later. Shown is a representative hematoxylin and eosin (H&E) image from 15 high-powered field views, selected by diagnostic clinical pathologists. Bar denotes approximately 100  $\mu\text{m}$ . Pre-TIL biopsy comprises 5 separate preserved blocks from 1 tumor from a single procedure performed on one day. Post-TIL biopsy comprises 3 core needle samples obtained from 4 total passes from a single procedure performed on one day. Each somatic mutation count represents 1 biologically independent sample.



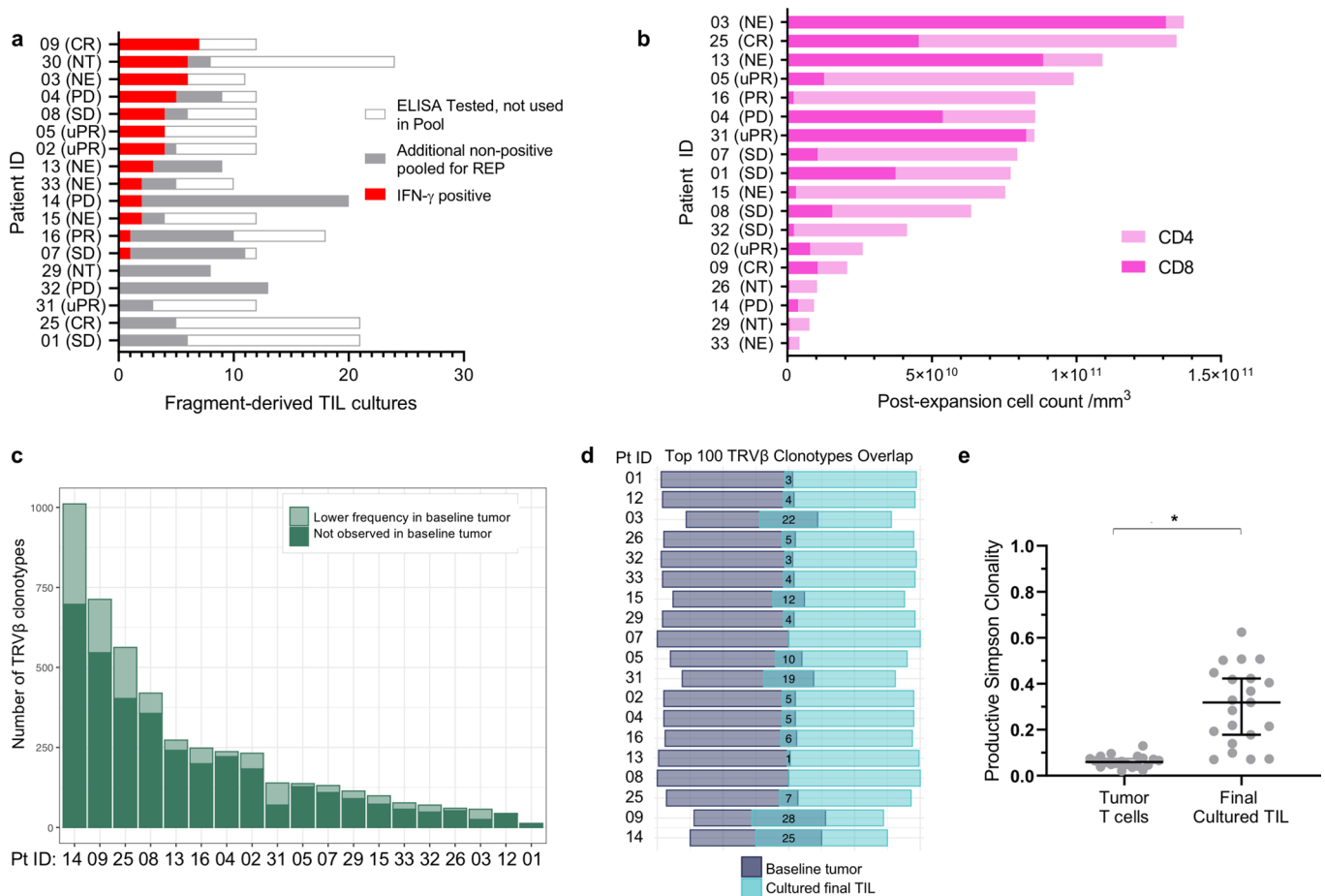
**Extended Data Fig. 7 | Overall survival from enrollment.** **a**, Overall survival of all enrolled patients ( $n=20$ ) from date of enrollment. **b**, Overall survival of patients who had not received any anti-cancer systemic therapy prior to enrollment ( $n=12$ ), and **c**, of patients who had received at least one line of previous systemic therapy ( $n=8$ ). Hashmarks denote 95% confidence intervals for survival probability. All patients were assessed for survival through the data cut-off of 10 Sept. 2020.



**Extended Data Fig. 8 | *In vitro* expansion of autologous T-cell clonotypes after stimulation with peptide antigens.** Clonotypes with significant increase using autologous T and dendritic cells from **a**, Patient 25 and **b**, Patient 9. T cells were co-cultured with autologous dendritic cells for 10 days and compared to controls wells including T cells only and no peptides. TCR V $\beta$  CDR3 AA denotes T-cell receptor V $\beta$  complementarity-determining region 3 amino acid. Fold expansion is relative to baseline control without peptide.



**Extended Data Fig. 9 | Expression of immune checkpoint ligands and cell composition of final infused TIL product. a**, Expression of immune checkpoint and cell activation markers assessed by flow cytometry as a proportion of either CD4<sup>+</sup> or CD8<sup>+</sup> T cells ( $n=18$  patients with 1 biologically independent experiment per patient, bar denotes median). **b**, Proportion of regulatory T cells (CD4<sup>+</sup> CD25<sup>+</sup> CD127<sup>dim</sup>). ( $n=18$  patients with 1 biologically independent experiment per patient). **c**, TIL cell population stratified by t-distributed stochastic neighbor embedding (t-SNE) mapping of memory differentiation subsets. Defined cell populations were assigned specific colors. Each patient is labeled by Pt ID. There are 18 patients presented in total, with 1 biologically independent experiment per patient.



**Extended Data Fig. 10 | Phenotype and clonotype features of final infused TIL.** **a**, Best overall response (BORR) and proportion of tumor-specific fragments in the final product. All patients with sufficient TIL for autologous reactivity testing performance are shown ( $n=18$ ). Pt 26 had insufficient tumor digest for autologous reactivity testing, and Pt 12 had insufficient pre-REP TIL for testing. A proportion were tested for reactivity with autologous tumor suspension using ELISA for interferon- $\gamma$ . Pink is the proportion of autologous-reactively cultures pooled for the final rapid expansion. Gray are either non-specific or negative cultures added to the pool, to ensure sufficient starting cell numbers. **b**, Patient BORR and dose of CD8<sup>+</sup> or CD4<sup>+</sup> cells in final expanded TIL product. All patients with final manufactured TIL are shown ( $n=18$ ). Pt 30 pre-REP TIL is still cryopreserved, and Pt 12 had insufficient pre-REP TIL to manufacture. 48 minced tumor fragments were cultured in IL-2. **c**, Change in T cell clonotypic composition between original intratumor T cells and final infused TIL. Across patients, there were variable numbers of enriched clones in the TIL culture, with a range 13 to 1011 clones. A large proportion of clones in each patient were not detected in the baseline tumor. **d**, Comparison of the most prevalent one hundred clones in the manufactured TIL culture with baseline tumor, with total number shown on the x-axis and overlap in middle. High repertoire turnover during TIL culture was observed in most samples. Several cultures shared no high frequency clones with their baseline tumors. **e**, Productive clonality Simpson clonality increased from baseline tumor to final cultured TIL (Exact  $p=0.000013$ , two-sided Wilcoxon signed rank test). Shown is the median and 95% confidence interval overlaying the individual values. All patients with manufactured TIL are shown ( $n=19$ ). Abbreviations: NT; not treated. NE; not evaluable. uPR, unconfirmed partial response.

## Reporting Summary

Nature Research wishes to improve the reproducibility of the work that we publish. This form provides structure for consistency and transparency in reporting. For further information on Nature Research policies, see our [Editorial Policies](#) and the [Editorial Policy Checklist](#).

### Statistics

For all statistical analyses, confirm that the following items are present in the figure legend, table legend, main text, or Methods section.

n/a Confirmed

- The exact sample size ( $n$ ) for each experimental group/condition, given as a discrete number and unit of measurement
- A statement on whether measurements were taken from distinct samples or whether the same sample was measured repeatedly
- The statistical test(s) used AND whether they are one- or two-sided  
*Only common tests should be described solely by name; describe more complex techniques in the Methods section.*
- A description of all covariates tested
- A description of any assumptions or corrections, such as tests of normality and adjustment for multiple comparisons
- A full description of the statistical parameters including central tendency (e.g. means) or other basic estimates (e.g. regression coefficient) AND variation (e.g. standard deviation) or associated estimates of uncertainty (e.g. confidence intervals)
- For null hypothesis testing, the test statistic (e.g.  $F$ ,  $t$ ,  $r$ ) with confidence intervals, effect sizes, degrees of freedom and  $P$  value noted  
*Give  $P$  values as exact values whenever suitable.*
- For Bayesian analysis, information on the choice of priors and Markov chain Monte Carlo settings
- For hierarchical and complex designs, identification of the appropriate level for tests and full reporting of outcomes
- Estimates of effect sizes (e.g. Cohen's  $d$ , Pearson's  $r$ ), indicating how they were calculated

*Our web collection on [statistics for biologists](#) contains articles on many of the points above.*

### Software and code

Policy information about [availability of computer code](#)

**Data collection** OnCore CTMS Enterprise Research system (Windows) was used to collect adverse events and for data outcome reporting. FlowJo software package v\_10.0 and 10.6.1 (Windows, English) was used to collect and analyze cell populations.

**Data analysis** Data were analyzed in R version 3.6.3 (2020-02-29), using Windows 10 x64 operating system, ming w32, user interface "RTerm" language English, United States, and Prism 9.0 (121) October 22, 2020. FEST analysis <http://www.stat-apps.onc.jhmi.edu/FEST/> version 2018-05-22. Adaptive Biotechnologies immunoSEQ analyzer version 3.0 was used to track clones and assess clonality of T cells. ELISA absorbance data was analyzed using SkanIt Software 4.1. STAR: ultrafast universal RNA-seq aligner was accessed as free open source software from <http://code.google.com/p/rna-star/>. Fusioncatcher Versions 1.0, and Version 1.20 -- November 8, 2019 were used for genomic analysis.

For manuscripts utilizing custom algorithms or software that are central to the research but not yet described in published literature, software must be made available to editors and reviewers. We strongly encourage code deposition in a community repository (e.g. GitHub). See the Nature Research [guidelines for submitting code & software](#) for further information.

### Data

Policy information about [availability of data](#)

All manuscripts must include a [data availability statement](#). This statement should provide the following information, where applicable:

- Accession codes, unique identifiers, or web links for publicly available datasets
- A list of figures that have associated raw data
- A description of any restrictions on data availability

Source data on expression, allelic frequency, and predicted MHC affinity for all identified neoantigens are provided in the supplemental excel spreadsheet uploaded as tab S4. TRVB information for 20 patients are available as the project "TIL trial for NSCLC" in the immuneACCESS public database: <https://clients.adaptivebiotech.com/immuneaccess>. Tumor whole exome sequencing and RNA-Seq raw data files (accession code: phs002486) is available in the public NIH

dbGaP data browser [https://www.ncbi.nlm.nih.gov/projects/gap/gap/cgi-bin/preview1.cgi?GAP\\_phis\\_code=UgsrhvZ3dGC4uQSh](https://www.ncbi.nlm.nih.gov/projects/gap/gap/cgi-bin/preview1.cgi?GAP_phis_code=UgsrhvZ3dGC4uQSh). The study protocol is uploaded as a supplementary file. In such circumstances that source data is not inferred from specified Tables/Figures, it is available upon request as a comma-delimited format from the study authors.

## Field-specific reporting

Please select the one below that is the best fit for your research. If you are not sure, read the appropriate sections before making your selection.

Life sciences     Behavioural & social sciences     Ecological, evolutionary & environmental sciences

For a reference copy of the document with all sections, see [nature.com/documents/nr-reporting-summary-flat.pdf](https://www.nature.com/documents/nr-reporting-summary-flat.pdf)

## Life sciences study design

All studies must disclose on these points even when the disclosure is negative.

Sample size	The trial sample size justification is described in the study protocol, page 59. We expected a total of 14 evaluable patients for the study. Sample size justification was based on continuous monitoring for toxicity using a Pocock-type stopping boundary. We consider the maximum-tolerated toxicity would be 17%. We considered the probability of early stopping to be at most 10%. With 14 patients, these settings resulted in a Pocock-type stopping boundary (Table A1 of Protocol). This boundary is equivalent to testing the null hypothesis, after each patient, that the maximum-tolerated toxicity rate is equal to 17%, using a one-sided level 0.053 test.
Data exclusions	No data is specifically excluded from each analysis. Data is omitted in sections where no data was available. Specifically, Pt 13 and 15 did not receive a measurable post-TIL CT scan and Pt 03 did not have a RECIST evaluable tumor lesion post-TIL. A data cutoff of September 2020 was applied for adverse events, survival time, sample collection, and response analysis. Timepoints with evaluable biosamples are indicated in Extended Data Table 2. Because of variations in sample collections for some patients, "Week 10" and "Week 20" permitted timepoints from +/-3 weeks.
Replication	Genomics was performed once on one biological sample each. Genomics could not be repeated due to expense of sequencing and availability of tumor sample. ELISpot or ELISA experiments were performed once with triplicate wells, on one biological sample each, and performed twice if sufficient sample was available. The replication was consistent with both experiments and successful.
Randomization	Not relevant, as no treatment types were compared. No randomization was used in this single-arm study.
Blinding	Not relevant in regards to treatment assignment, since all patients received the same treatment on an open-label trial. In regards to comparison of biomarkers, the pathologist Dr James Sallman reviewed tumor markers such as CD3+ staining without prior knowledge of patient outcomes. Because biomarkers were neither a primary or secondary endpoint of the trial, no formal blinding program was implemented.

## Reporting for specific materials, systems and methods

We require information from authors about some types of materials, experimental systems and methods used in many studies. Here, indicate whether each material, system or method listed is relevant to your study. If you are not sure if a list item applies to your research, read the appropriate section before selecting a response.

### Materials & experimental systems

n/a	Involved in the study
<input type="checkbox"/>	<input checked="" type="checkbox"/> Antibodies
<input checked="" type="checkbox"/>	<input type="checkbox"/> Eukaryotic cell lines
<input checked="" type="checkbox"/>	<input type="checkbox"/> Palaeontology and archaeology
<input checked="" type="checkbox"/>	<input type="checkbox"/> Animals and other organisms
<input type="checkbox"/>	<input checked="" type="checkbox"/> Human research participants
<input type="checkbox"/>	<input checked="" type="checkbox"/> Clinical data
<input checked="" type="checkbox"/>	<input type="checkbox"/> Dual use research of concern

### Methods

n/a	Involved in the study
<input checked="" type="checkbox"/>	<input type="checkbox"/> ChIP-seq
<input type="checkbox"/>	<input checked="" type="checkbox"/> Flow cytometry
<input checked="" type="checkbox"/>	<input type="checkbox"/> MRI-based neuroimaging

## Antibodies

Antibodies used	Flow cytometry antibody / Catalogue/ Lot Number were: Anti- Human Tim-3 (CD366) BV421 565562 8165981 Anti- Human TIGIT PE-Cy™7 25-9500-42 1995496 Anti- Human LAG3 (CD223) PE 565616 8281624 Anti- Human CD95 BV711 563132 8288847 Anti- Human CD8 BUV395 563795 8220831 Anti- Human CD56 BUV563 565704(Discontinued)/612928 9022780 Anti- Human CD45RA FITC 555488 7055682 Anti- Human CD4 BUV737 564305(Discontinued)/612748 8310934
-----------------	--

Anti- Human CD314 (NGK2D) APC 558071 8159562  
 Anti- Human CD3 BUV496 564809(Discontinued)/612940 8296578  
 Anti- Human CD28 BV480 566110 7054585  
 Anti- Human CD279 (PD-1) BV480 566112 7171905  
 Anti- Human CD272 (BTLA) APC 564800 7150655  
 Anti- Human CD27 PerCP-Cy™5.5 560612 8138674  
 Anti- Human CD25 PerCP-Cy™5.5 560503 8339603  
 Anti- Human CD244 FITC 550815 6307734  
 Anti- Human CD226 BV711 564796 7205804  
 Anti- Human CD197 (CCR7) BV421 562555 8291773  
 Anti- Human CD195 BV786 565001 8353941  
 Anti- Human CD194 PE-Cy™7 557864 7250981  
 Anti- Human CD19 BV605 562653 8281951  
 Anti- Human CD152 BV786 563931 8129674  
 Anti- Human CD14 BV605 564054 8194956  
 Anti- Human CD127 PE 557938 7242866;  
 All from BD Biosciences.

The optimized dilutions for the flow cytometry antibodies included:

NGK2D 1:5; CD197 1:10; CD56 1:20; CD195 1:20; CD45RA 1:20; CD194 1:20; CD3 1:50; CD4 1:50' CD14 1:50; CD19 1:50; CD25 1:50; CD95 1:50; CD8 1:100; CD28 1:100; CD127 1:150; CD244 1:05; CD152 1:20; CD223 1:20; CD366 1:20; CD3 1:50; CD4 1:50; CD14 1:50; CD19 1:50; CD279 1:50; CD226 1:50; TIGIT 1:50; CD8 1:100; CD272 1:100; CD27 1:100.

Rainbow Calibration Particles (3.0 - 3.4 µm) from BD Biosciences was used for calibration of flow cytometry between runs.

Human IFN-γ Immunoassay (R&D Systems) Catalog Number DIF50 was used for autologous reactivity testing of TIL cultures, this kit includes a polyclonal antibody specific for human IFN-γ. Dynabeads Human T-Activator CD3/CD28/CB137 antibody from Gibco cat # 11163D was used to activate T cells for ELISA. OKT3 (14-0037-82) from Thermo Fisher Scientific was used as positive control for T cell stimulation for ELISpot.

For immunohistochemical detection of PD-L1, the PD-L1 22C3 mouse anti-human monoclonal antibody (SK 006, Agilent) was performed according to manufacturer guidelines utilizing the DAKO EnVision FLEX visualization system on the DAKO Autostainer Link 48 on formalin paraffin embedded tissue. The interpretation of stained tumor cells are analyzed by manual morphometric analysis and reported using the Tumor Proportion Score (TPS), which is the percentage of viable tumor cells showing partial or complete membrane staining.

#### Validation

A Certificate of Analysis showing compliance with all BDB release criteria for flow cytometry, using Human FC Optimal Conc µg/Test (0.500 - 1.000) was confirmed for each of the BD antibody catalogue and lot number combinations listed above. These certificates are publically available at <https://regdocs.bd.com/regdocs/qcSearchResults>. For the flow cytometry antibodies, the CD-Chex Plus (Streck) control (Lots #73030071, 90210071) for internal validation was run for each patient during TIL analysis for CD3, CD4, and CD8.

For immunohistochemical detection of PD-L1 using 22C3 antibody, the Moffitt pathology laboratory is regulated under the Clinical Laboratory Improvement Amendments of 1988 (CLIA 1988) pursuant to the requirements of CLIA, and verified the test's accuracy, precision, reportable range of patient test results, reference range, analytical specificity and sensitivity, and other relevant performance specifications.

## Human research participants

Policy information about [studies involving human research participants](#)

#### Population characteristics

This information is provided in Table 1.

#### Recruitment

All participants were recruited by medical oncology or surgeons within a Thoracic multi-disciplinary clinic setting at Moffitt Cancer Center, which has a catchment area of the surrounding 10 counties of Florida. The clinic demographic consists primarily of suburban and urban Caucasian patients with health insurance access. Only two of 20 enrolled patients were African American. Spanish language consent was available for translation within the study budget, however no enrolled patients were primary Spanish language speakers. No sources of recruitment bias were identified.

#### Ethics oversight

This study was approved by Adverra Institutional Review Board (FWA 0023875) and underwent FDA safety review (IND 17489).

Note that full information on the approval of the study protocol must also be provided in the manuscript.

## Clinical data

Policy information about [clinical studies](#)

All manuscripts should comply with the ICMJE [guidelines for publication of clinical research](#) and a completed [CONSORT checklist](#) must be included with all submissions.

#### Clinical trial registration

NCT03215810

#### Study protocol

Full study protocol is uploaded as a supplemental file.

#### Data collection

Patients were accrued from October 2017 to January 2020. Data analysis was performed with data cutoff 10 Sept 2020. OnCore CTMS Enterprise Research system (Windows) was used to collect adverse events and for data outcome reporting. Data was collected in tumor measurement worksheets by assigned MCC 19122 trial data managers at Moffitt Cancer Center. Data managers collected and graded adverse events based on review of the clinical charts from enrolled patients. Adverse event attribution was performed based on source documentation and the treating physicians. CT scans were conducted every 6 weeks, followed by every 12 weeks

after completion of therapy, according to the study calendar, at the cancer center. Target lesion assignment and measurements per RECIST v1.1 were performed and included within the primary radiology report by the interpreting radiologists. Tumor measurement worksheets were completed by the clinical trial coordinators and signed by the treating physicians. Blood samples were collected according to the study calendar.

## Outcomes

The primary objective of the study was to demonstrate that treatment with nivolumab in patients undergoing lymphodepletion/TIL/IL2 therapy was safe, with a continuous Pocock-type stopping boundary for serious toxicity of < 17%, with safety reported based upon CTCAE version 4.0 criteria. Our hypothesis the combination of TIL therapy and nivolumab for NSCLC patients will be feasible and achieve an acceptable toxicity profile. The secondary objectives were to 1) evaluate the efficacy of TIL administered in combination with nivolumab in subjects with NSCLC by assessing the objective response rate (ORR) per RECIST v1.1; 2) to evaluate the efficacy of TIL administered in combination with nivolumab in subjects with NSCLC by assessing duration of response (DoR); 3) to evaluate the T-cell persistence following TIL and nivolumab when administered in combination, using T cell phenotype such as CDR3 sequencing.

## Flow Cytometry

### Plots

Confirm that:

- The axis labels state the marker and fluorochrome used (e.g. CD4-FITC).
- The axis scales are clearly visible. Include numbers along axes only for bottom left plot of group (a 'group' is an analysis of identical markers).
- All plots are contour plots with outliers or pseudocolor plots.
- A numerical value for number of cells or percentage (with statistics) is provided.

### Methodology

Sample preparation

Patients had peripheral blood draw in 10 mL sodium heparin tubes, which was then separated on a Ficoll gradient and cryopreserved in albumin and DMSO.

Instrument

BD Symphony

Software

Flowjo v10.6.1

Cell population abundance

After cell sorting, we run flow cytometry on sorted populations to determine cell purity. Only post-sort populations with purity more than 95% will be used for the experiments (e.g. immunoseq in this manuscript).

Gating strategy

From FSC/SSC plots, we gated lymphocytes and only gated single cells using FSC-A/FSC-H and SSC-A/SSC-H. Then CD3+ Zombie NIR- CD14/CD19- cells were gated as live CD3+ cells, where CD4+ and CD8+ T cells were gated respectively. The following T cell differentiation subsets were gated within each of CD4 or CD8 T cells: naive T cells--CCR7+CD45RA+CD95-, Tscm--CCR7+CD45RA+CD95+, Tcm--CCR7+CD45RA-, Tem--CCR7-CD45RA-, Teff--CCR7-CD45RA+. Positive and negative populations were identified using FMO controls. A figure showing an example of our gating strategy is provided in the supplementary data.

- Tick this box to confirm that a figure exemplifying the gating strategy is provided in the Supplementary Information.